Chiral primordial gravitational waves from dilaton induced delayed chromonatural inflation

Obata, Ippei

Soda, Jiro

(Citation)
Physical Review D,93(12):123502-123502

(Issue Date)
2016-06-01

(Resource Type)
journal article

(Version)
Version of Record

PHYSICAL REVIEW D **93,** 123502 (2016)

Chiral primordial gravitational waves from dilaton induced delayed chromonatural inflation

Ippei Obata[1,2,*] and Jiro Soda[2,†]
(CLEO Collaboration)

[1]Department of Physics, Kyoto University, Kyoto 606-8502, Japan
[2]Department of Physics, Kobe University, Kobe 657-8501, Japan
(Received 29 February 2016; published 1 June 2016)

We study inflation driven by a dilaton and an axion, both of which are coupled to a SU(2) gauge field. We find that the inflation driven by the dilaton occurs in the early stage of inflation during which the gauge field grows due to the gauge-kinetic function. When the energy density of magnetic fields catches up with that of electric fields, chromonatural inflation takes over in the late stage of inflation, which we call delayed chromonatural inflation. Thus, the delayed chromonatural inflation driven by the axion and the gauge field is induced by the dilaton. The interesting outcome of the model is the generation of chiral primordial gravitational waves on small scales. Since the gauge field is inert in the early stage of inflation, it is viable in contrast to the conventional chromonatural inflation. We find the parameter region where chiral gravitational waves are generated in a frequency range higher than nHz, which are potentially detectable in future gravitational wave interferometers and pulsar-timing arrays such as DECi-hertz Interferometer Gravitational wave Observatory (DECIGO), evolved Laser Interferometer Space Antenna (eLISA), and Square Kilometer Array (SKA).

DOI: 10.1103/PhysRevD.93.123502

I. INTRODUCTION

Primordial fluctuations of matter produced quantum mechanically during inflation [1] elegantly explain the origin of the cosmic microwave background (CMB) anisotropy and the large-scale structure of our present Universe. On top of the primordial fluctuations of matter, it is well known that inflation quantum mechanically generates fluctuations of spacetime, so-called primordial gravitational waves. The current constraint on the amplitude of primordial gravitational waves in terms of the tensor-to-scalar ratio r comes from the observation of the CMB. The latest joint analysis of the BICEP2/Keck Array and Planck data provided an upper limit on the tensor-to-scalar ratio as $r|_{0.05} < 0.07$ at 95% confidence level [2,3]. Remarkably, the amplitude of primordial gravitational waves is directly related to the energy scale of inflation. The energy scale probed by the CMB observations is around the scale of grand unification theory (GUT), 10^{16} GeV. Hence, once primordial gravitational waves were detected, they would be a powerful probe of the physics in the early Universe such as the GUT, supergravity, and superstring theory.

From the perspective of the rapid progress of cosmological observations, it is necessary to adapt inflation to the percent-level precision of observations. This should be done based on fundamental theory. As a consequence, it is expected that qualitatively new phenomena in inflation are found, and those should be probed by primordial gravitational waves. Since supergravity is the low-energy limit of superstring theory and the GUT might be embedded into supergravity, it is legitimate to investigate inflation based on supergravity. Indeed, there have been a lot of efforts to construct models based on supergravity [4]. However, in the previous study, the gauge sector in supergravity has been overlooked. In fact, it was legitimate to truncate the gauge sector because it apparently gives rise to tiny effects on observables. From the point of view of precision cosmology, however, it is worth exploring the role of the gauge sector in inflation. In supergravity, there exists a complex scalar field; we call its real part a dilaton and its imaginary part an axion. These two scalar fields are candidates for an inflaton, and their couplings to the gauge sector are of interest to us.[1] There are two ways in which an inflaton field is coupled to the gauge field. One is the dilaton coupling to the gauge field through a gauge-kinetic function. The other is an axion coupling to the gauge field. Thus, the issue to be clarified is if we can probe the gauge sector in inflation with the primordial gravitational waves.

Once we introduce the dilaton field and its gauge-kinetic function, there are interesting phenomenologies such as the

*obata@tap.scphys.kyoto-u.ac.jp
†jiro@phys.sci.kobe-u.ac.jp

[1]Even in nonsupersymmetric models, it is worth studying the role of such a gauge-kinetic function in the early Universe since it naturally appears when we consider radiative corrections of charged scalar fields, models obtained by dimensional reduction from higher dimensions, and so on.

generation of primordial magnetic fields [5]. In particular, recently, it has been found that a nontrivial gauge-kinetic function could trigger the growth of the gauge field which stops at the saturating point and the amplitude of the gauge field is sustained during inflation [6]. The surviving gauge field results in the statistical anisotropy in the primordial fluctuations [7,8]. In the Abelian gauge field cases, it accompanies anisotropic inflation [6,9]. In the non-Abelian gauge field cases, the isotropic configuration is an attractor [10]. However, since its convergence is quite slow, the statistical anisotropy depending on the initial conditions would appear [11,12]. Thus, we can expect the cross-correlation between gravitational waves and curvature perturbations on top of the statistical anisotropy in the autocorrelation of gravitational waves [8]. It is also possible to generate gravitational waves from the particle production of gauge fields by the dilaton [13].

In the presence of the axion coupling during inflation, there occurs the transient tachyonic instability in one of helicity modes of the gauge field near the horizon crossing. Remarkably, the parity-violating gauge field produces the circular polarization of gravitational waves, namely, chiral gravitational waves [14–25]. We can test this interesting outcome by observing the correlation between CMB temperature anisotropy and B-mode polarization [26–28] or by analyzing the residual signal of pulsar-timing arrays [29]. In the case of the Abelian gauge field, however, the gauge field also produces curvature perturbations with large non-Gaussianity. As a result, this effect easily violates the current observational bounds on the non-Gaussianity of the CMB anisotropies [14,15,30–32]. More seriously, the strong interaction of the axion to the gauge field breaks perturbative descriptions in the in-in formalism [33]. These constraints severely constrain amplitudes of chiral gravitational waves and make them invisible on CMB scales. In the case of the non-Abelian gauge field, there is another effect of the axion coupling. Indeed, the interaction of the axion with the non-Abelian gauge field gives rise to an effective Hubble friction and generates a slow-roll inflationary solution for a wide range of parameters [34] (see also related models [35]). In the presence of the background gauge field, the non-Abelian gauge field perturbations have tensor perturbations, and one of circular polarization states experiences the tachyonic instability near the horizon crossing, which produces chiral gravitational waves. However, this inflation model is in conflict with CMB observations because either the spectral index of the curvature perturbations is too red or gravitational waves are produced too much [22–24]. This result stems from the fact that the strength of the interaction between the axion and the gauge field is almost constant during inflation. Hence, sizable chiral primordial gravitational waves cannot be reconciled with the constraints on CMB scales.

As we have explained in the above, recent works have revealed roles of two types of the coupling between the inflaton and the gauge field separately. From the point of view of supergravity, however, we should incorporate both the dilaton and the axion into a model at the same time. In this paper, we will focus on this possibility and find a novel effect induced by the presence of both couplings, which can be probed by primordial gravitational waves. The point is that the gauge-kinetic function of the dilaton makes the gauge field increase and controls the strength of the axion-gauge field interaction. For initial conditions, we choose the gauge field small enough so that we can ignore an effective coupling of the axion to the gauge field in the early stage of inflation. Therefore, the tachyonic instability plays no role when primordial fluctuations on CMB scales are generated. However, the gauge field grows due to the dilaton coupling through the gauge-kinetic function until the nonlinear effect of the gauge field appears in the background dynamics. Eventually, the gauge field settles in an attractor and realizes delayed chromonatural inflation [34] in the late stage of inflation, Remarkably, sizable chiral gravitational waves are generated only on small scales, the amplitude of which can be detectable by future space interferometers and pulsar-timing arrays such as DECIGO, eLISA, and SKA [36–38].

This paper is organized as follows. In Sec. II, we present an inflation model with a dilaton and an axion, both of which are coupled with a SU(2) gauge field. We then derive equations of motions for the homogeneous fields and study the background dynamics. We show that two different inflationary stages are realized in Sec. II A. In Sec. III, first we decompose perturbations into scalar, vector, and tensor perturbations and give the gauge conditions. Next, we analyze tensor dynamics and show that chiral gravitational waves are produced on scales smaller than CMB scales. In Sec. IV, we also discuss the dynamics of scalar perturbations. We estimate the amplitude of curvature perturbations on CMB scales and check the stability of scalar dynamics on small scales. In Sec. V, we discuss phenomenological predictions in this model. The final section is devoted to the conclusion. In the Appendix, we list equations used in the numerical calculations.

II. INFLATION MODEL WITH DILATON AND AXION COUPLED TO SU(2) GAUGE FIELD

In this section, we present an inflationary model and derive equations of background motions. Specifically, we consider a dilaton field φ and an axion field σ, both of which are coupled with an SU(2) gauge field A^a_μ. The field strength of the gauge field $F^a_{\mu\nu}$ is defined by

$$F^a_{\mu\nu} = \partial_\mu A^a_\nu - \partial_\nu A^a_\mu + g\epsilon^{abc} A^b_\mu A^c_\nu, \tag{1}$$

where g is its gauge coupling constant and ϵ^{abc} is the Levi-Civitá symbol of which the components are structure constants of the SU(2) gauge field. The dual field strength tensor $\tilde{F}^{a\mu\nu}$ is defined by

$$\tilde{F}^{a\mu\nu} = \frac{1}{2!}\sqrt{-g}\epsilon^{\mu\nu\rho\sigma}F^a_{\rho\sigma},$$
$$\epsilon^{0123} = g^{0\alpha}g^{1\beta}g^{2\gamma}g^{3\delta}\epsilon_{\alpha\beta\gamma\delta} = \frac{1}{-g}, \tag{2}$$

where $\epsilon_{\mu\nu\rho\sigma}$ is an antisymmetric tensor. The action reads

$$\begin{aligned} S &= S_{\rm EH} + S_{\rm dilaton} + S_{\rm axion} + S_{\rm gauge} + S_{\rm CS} \\ &= \int dx^4 \sqrt{-g}\bigg[\frac{1}{2}R - \frac{1}{2}(\partial_\mu\varphi)^2 - V(\varphi) - \frac{1}{2}(\partial_\mu\sigma)^2 \\ &\quad - W(\sigma) - \frac{1}{4}I(\varphi)^2 F^{a\mu\nu}F^a_{\mu\nu} - \frac{1}{4}\lambda\frac{\sigma}{f}\tilde{F}^{a\mu\nu}F^a_{\mu\nu}\bigg], \end{aligned} \tag{3}$$

where we used units $\hbar = c = 1$ and $M_{\rm pl} = (8\pi G)^{-1/2} = 1$. Here, g is a determinant of a metric $g_{\mu\nu}$ (note that it is not related with the gauge coupling constant), R is a Ricci scalar, and f is a decay constant of the axion. Moreover, we introduced a coupling constant of the axion to the gauge field λ. We have also introduced the potential functions $V(\varphi)$ and $W(\sigma)$.

As to the metric, we adapt the Arnowitt-Deser-Misner parametrization

$$ds^2 = -N^2dt^2 + q_{ij}(dx^i + N^i dt)(dx^j + N^j dt), \tag{4}$$

where N is a lapse function and N^i is a shift function, which are Lagrange multipliers of the system. An induced metric q_{ij} on the three-dimensional spatial hypersurface is used to raise or lower the index as

$$q^{ik}q_{kj} = \delta^i_j, \qquad N^i = q^{ij}N_j. \tag{5}$$

Thus, the metric can be expressed by

$$g_{\mu\nu} = \begin{pmatrix} -N^2 + N_iN^i & N_j \\ N_i & q_{ij} \end{pmatrix},$$
$$g^{\mu\nu} = \begin{pmatrix} -N^{-2} & N^{-2}N^j \\ N^{-2}N^i & q^{ij} - N^{-2}N^iN^j \end{pmatrix}. \tag{6}$$

Using these variables, we can rewrite the action (3) as

$$S_{\rm EH} = \int dx^4 N\sqrt{q}\left[\frac{1}{2}({}^{(3)}R + K_{ij}K^{ij} - K^2)\right], \tag{7}$$

$$\begin{aligned} S_{\rm dilaton} = \int dx^4 N\sqrt{q}\bigg[&\frac{1}{N^2}\left(\frac{1}{2}\dot{\varphi}^2 - N^i\dot{\varphi}\varphi_{,i} + \frac{1}{2}(N^i\varphi_{,i})^2\right) \\ &- \left(\frac{1}{2}q^{ij}\varphi_{,i}\varphi_{,j} + V(\varphi)\right)\bigg], \end{aligned} \tag{8}$$

$$\begin{aligned} S_{\rm axion} = \int dx^4 N\sqrt{q}\bigg[&\frac{1}{N^2}\left(\frac{1}{2}\dot{\sigma}^2 - N^i\dot{\sigma}\sigma_{,i} + \frac{1}{2}(N^i\sigma_{,i})^2\right) \\ &- \left(\frac{1}{2}q^{ij}\sigma_{,i}\sigma_{,j} + W(\sigma)\right)\bigg], \end{aligned} \tag{9}$$

$$\begin{aligned} S_{\rm gauge} = \int dx^4 N\sqrt{q}\bigg[&\frac{1}{2N^2}I(\varphi)^2 q^{ik}(F^a_{0i} + F^a_{ij}N^j) \\ &\times (F^a_{0k} + F^a_{kl}N^l) - \frac{1}{4}I(\varphi)^2 q^{ik}q^{jl}F^a_{ij}F^a_{kl}\bigg], \end{aligned} \tag{10}$$

$$S_{\rm CS} = \int dx^4\left[-\frac{1}{2}\lambda\frac{\sigma}{f}\epsilon^{ijk}F^a_{0i}F^a_{jk}\right]. \tag{11}$$

Note that Chern-Simons interaction does not include metric variables. Here, q is a determinant of the metric q_{ij}. We defined the extrinsic curvature of a hypersurface

$$K_{ij} \equiv \frac{1}{2N}(\dot{q}_{ij} - 2N_{(i|j)}) \tag{12}$$

and the Ricci scalar of the hypersurface

$${}^{(3)}R = (q_{ij,kl} + q_{mn}{}^{(3)}\Gamma^m_{ij}{}^{(3)}\Gamma^n_{kl})(q^{ik}q^{jl} - q^{ij}q^{kl}), \tag{13}$$

where

$${}^{(3)}\Gamma^i_{jk} = \frac{1}{2}q^{il}(q_{lj,k} + q_{lk,j} - q_{jk,l}). \tag{14}$$

Let us consider the homogeneous background dynamics in this setup. For the metric, we use a spatially flat metric

$$N = N(t), \qquad N_i = 0, \qquad q_{ij} = a(t)^2\delta_{ij}. \tag{15}$$

After taking the variation of the action, we set $N(t) = 1$. Thus, the time function t becomes the cosmic time. For the dilaton and the axion, we take homogeneous configurations $\varphi = \varphi(t), \quad \sigma = \sigma(t)$. For a gauge condition, we choose the temporal gauge

$$A^a_0 = 0. \tag{16}$$

We also take an ansatz,

$$A^a_i = A(t)\delta^a_i = a(t)Q(t)\delta^a_i, \tag{17}$$

which is invariant under the diagonal transformation of the spatial rotation SO(3) and the SU(2) gauge symmetry. Note that $Q(t)$ is a scalar under the diagonal transformation, and we use this variable later. Thus, their field strength $F^a_{\mu\nu}$ can be deduced as

$$F^a_{0i} = \frac{dA}{dt}\delta^a_i \equiv aE(t)\delta^a_i,$$
$$F^a_{ij} = g\epsilon^{abc}A^b_iA^c_j = gA^2\epsilon^a_{ij} \equiv a^2B(t)\epsilon^a_{ij}, \tag{18}$$

where we defined electric and magnetic components $E(t)$ and $B(t)$. Substituting these configurations into the action, we obtain the background action

$$S = \int d^4x \frac{a^3}{N}\left[-3\frac{\dot{a}^2}{a^2} + \frac{1}{2}\dot{\varphi}^2 - N^2 V + \frac{1}{2}\dot{\sigma}^2 - N^2 W + \frac{3}{2}I^2(E^2 - N^2B^2) - 3N\frac{\lambda}{f}\sigma EB\right], \tag{19}$$

where a dot denotes a derivative with respect to the cosmic time t. Taking the variation with respect to N and setting $N = 1$ after the variation, we obtain the Hamiltonian constraint

$$3H^2 = \frac{1}{2}\dot{\varphi}^2 + V + \frac{1}{2}\dot{\sigma}^2 + W + \rho_E + \rho_B, \tag{20}$$

where $H \equiv \dot{a}/a$ is the Hubble parameter. Here, we defined the following energy densities of electric and magnetic fields:

$$\rho_E \equiv \frac{3}{2}I^2E^2 = \frac{3}{2}I^2\frac{\dot{A}^2}{a^2}, \quad \rho_B \equiv \frac{3}{2}I^2B^2 = \frac{3}{2}I^2\frac{g^2A^4}{a^4}. \tag{21}$$

The equations for the dilaton, the axion, and the gauge field read

$$\ddot{\varphi} + 3H\dot{\varphi} + V_\varphi = 2\frac{I_\varphi}{I}(\rho_E - \rho_B), \tag{22}$$

$$\ddot{\sigma} + 3H\dot{\sigma} + W_\sigma = -3\frac{\lambda}{f}EB, \tag{23}$$

$$\ddot{A} + \left(H + 2\frac{\dot{I}}{I}\right)\dot{A} + 2g^2\frac{A^3}{a^2} = \frac{\lambda}{f}\dot{\sigma}g\frac{A^2}{aI^2}, \tag{24}$$

where

$$V_\varphi \equiv \frac{dV}{d\varphi}, \qquad W_\sigma \equiv \frac{dW}{d\sigma}, \qquad I_\varphi \equiv \frac{dI}{d\varphi}. \tag{25}$$

The equation for the scale factor $a(t)$ is given by

$$\dot{H} = -\left(\frac{1}{2}\dot{\varphi}^2 + \frac{1}{2}\dot{\sigma}^2 + \frac{2}{3}(\rho_E + \rho_B)\right). \tag{26}$$

Now that we have obtained the basic equations, we can discuss the inflationary dynamics.

A. Inflationary dynamics

In this section, we analyze the background dynamics which eventually produces chiral gravitational waves on small scales.

First, we discuss initial conditions. We assume that the dilaton is energetically dominant and plays the role of an inflaton in the early stage of inflation. The dynamics during inflation can be described by slow-roll equations

$$3H^2 \simeq V, \qquad 3H\dot{\varphi} + V_\varphi \simeq 0. \tag{27}$$

In addition to those, we assume that the axion also satisfies a slow-roll equation,

$$3H\dot{\sigma} + W_\sigma \simeq 0. \tag{28}$$

Now, we introduce the slow-roll parameters in this system,

$$\epsilon_H \equiv -\frac{\dot{H}}{H^2} = \epsilon_\varphi + \epsilon_\sigma + \epsilon_E + \epsilon_B, \tag{29}$$

$$\eta_H \equiv \frac{\dot{\epsilon}_H}{H\epsilon_H} = 2\left(\epsilon_H + \frac{\epsilon_\varphi}{\epsilon_H}\frac{\ddot{\varphi}}{H\dot{\varphi}} + \frac{\epsilon_\sigma}{\epsilon_H}\frac{\ddot{\sigma}}{H\dot{\sigma}} + \frac{\epsilon_E}{\epsilon_H}\left(\frac{\dot{I}}{HI} + \frac{\dot{E}}{HE}\right) + \frac{\epsilon_B}{\epsilon_H}\left(\frac{\dot{I}}{HI} + \frac{\dot{B}}{HB}\right)\right), \tag{30}$$

where we defined slow-roll parameters

$$\epsilon_\varphi \equiv \frac{1}{2}\frac{\dot{\varphi}^2}{H^2}, \qquad \epsilon_\sigma \equiv \frac{1}{2}\frac{\dot{\sigma}^2}{H^2}, \qquad \epsilon_E \equiv \frac{2}{3}\frac{\rho_E}{H^2}, \qquad \epsilon_B \equiv \frac{2}{3}\frac{\rho_B}{H^2}. \tag{31}$$

Here, we assume the relation $\epsilon_\sigma \ll \epsilon_H$, which can be realized easily. We can express the scale factor as a function of φ,

$$a \simeq a_0 \exp\left[-\int_0 \frac{V}{V_\varphi}d\varphi\right] = a(\varphi), \tag{32}$$

where the index 0 represents an initial value. Inspired by this result, we put the gauge-kinetic function as[2]

$$I(\varphi) = I_0 \exp\left[-n\int_0 \frac{V}{V_\varphi}d\varphi\right], \tag{33}$$

where I_0 is a constant. Thus, we have an approximate relation $I(\varphi) \propto a^n$ during slow-roll inflation. Note that n is a parameter and it controls the strength of the gauge coupling.

In this paper, we consider a gauge field with a weak coupling constant. Namely, $I(\varphi)$ is a decreasing function ($n < 0$), and we choose its initial value I_0 very large in order to get $g^{-1}I \sim \mathcal{O}(1)$ at the end of inflation. This assumption is necessary to avoid the strong coupling problem. Hence, the electric and magnetic components must be very small in order to satisfy slow-roll

[2]Note that this specific choice is due to the analytical convenience for our discussion below. In principle, we can consider a more general functional form for the gauge-kinetic function. We expect that the results do not change even for other choices as long as the functional shape is similar in the relevant range of the dilaton field.

equations (27). The naturalness of this requirement depends on the effective potential of the gauge field, as we discuss later. Because of this assumption, we can neglect non-linear terms in the EOM in early periods. Then, Eq. (24) can be reduced to

$$\ddot{A} + \left(H + 2\frac{\dot{I}}{I}\right)\dot{A} \simeq 0, \tag{34}$$

which can be integrated as

$$aI^2\dot{A} = \mathrm{const} \equiv C. \tag{35}$$

Thus, the energy density of the electric field evolves as

$$\rho_E = \frac{3C^2}{2a^4 I^2} \propto a^{-2(n+2)}. \tag{36}$$

Since we are interested in the solution in which the energy density of the gauge field does not decay, we consider the $n \leq -2$ region. On the other hand, the growing mode of the magnetic energy density is proportional to $a^{-2(3n+4)}$ so that ρ_B rows more rapidly than ρ_E. Therefore, we can separate the inflationary history of this model into two stages. In the early stage of inflation, ρ_B is negligibly small compared to ρ_E, so its effect on the dynamics can be ignored in the background motion. We assume that primordial fluctuations on CMB scales are generated during this stage. In the late stage of inflation, however, ρ_B grows sufficiently first and catches up with ρ_E. As we explicitly show later, during this stage, the interaction between the gauge field and the axion becomes important, and an inflationary dynamics goes into an attractor solution, which is quite similar to the dynamics of chromonatural inflation [34]. From now on, we explain these two inflationary stages separately.

1. Early stage of inflation

In an initial period, the energy density of the gauge field is so small that only a dilaton contributes an inflationary dynamics. However, when ρ_E grows sufficiently, the slow-roll condition for φ will no longer be valid and will be modified as

$$3H\dot{\varphi} + V_\varphi \simeq 2\frac{I_\varphi}{I}\rho_E. \tag{37}$$

Substituting Eq. (36) into Eq. (37), we can solve this equation [6] and find the gauge-kinetic function as

$$a^4 I^2 \simeq -\frac{n^2}{n+2}\frac{3C^2}{2\epsilon_V V}(1 + D_1 a^{2(n+2)}), \tag{38}$$

where D_1 is a constant of integration and $\epsilon_V \equiv \frac{1}{2}(\frac{V_\varphi}{V})^2$ is the slow-roll parameter in terms of the potential. Here, we note the relation

$$\epsilon_E \simeq -\frac{2(n+2)}{n^2}\epsilon_V. \tag{39}$$

We neglected the time dependence of $\epsilon_V V$ in the above. We can see that the second term in Eq. (38) soon becomes negligible when $n < -2$. Thus, ρ_E settles in a nearly constant value during this period,

$$\rho_E \simeq -\frac{n+2}{n^2}\epsilon_V V. \tag{40}$$

That implies the effective n goes to -2 [39]. At this time, the relation between ϵ_V and ϵ_φ reads

$$\sqrt{\epsilon_\varphi} \simeq \sqrt{\epsilon_V} + \frac{n\epsilon_E}{\sqrt{2\epsilon_V}}. \tag{41}$$

Remarkably, an electric component of the gauge field finally supports the slow-roll inflation in this period. Then, the Hubble slow-roll parameters read

$$\epsilon_H \simeq \epsilon_\varphi + \epsilon_E, \tag{42}$$

$$\eta_H \simeq 2\left(\epsilon_H + \frac{\epsilon_\varphi}{\epsilon_H}\frac{\ddot{\varphi}}{H\dot{\varphi}} + \frac{\epsilon_E}{\epsilon_H}\left(\frac{\dot{I}}{HI} + \frac{\dot{E}}{HE}\right)\right). \tag{43}$$

2. Late stage of inflation

Up to here, we have neglected the nonlinear effect of the gauge field. However, the energy density of magnetic field ρ_B grows and eventually becomes greater than ρ_E for $n \leq -2$. As the nonlinear effect becomes important, we cannot use Eq. (35). Instead, we have to consider the full equation of motion for the gauge field (24). Here, we rewrite Eq. (24) into the equation for Q defined by (17)

$$\ddot{Q} + \left(1 + \frac{2}{3}\frac{\dot{I}}{HI}\right)3H\dot{Q} = -\left(\left(2 - \epsilon_H + 2\frac{\dot{I}}{HI}\right)H^2 Q + 2g^2Q^3 - \frac{\lambda}{f}\dot{\sigma}\frac{gQ^2}{I^2}\right), \tag{44}$$

which looks like an equation for a scalar field. Hence, we can interpret the right-hand side of Eq. (44) as an effective potential force of the gauge field. It is easy to read off the effective potential from Eq. (44) as

$$U_{\mathrm{eff}}(Q) = \left(1 + \frac{\dot{I}}{HI}\right)H^2Q^2 - \frac{1}{3}\frac{\lambda}{f}\dot{\sigma}\frac{gQ^3}{I^2} + \frac{1}{2}g^2Q^4. \tag{45}$$

Note that we neglected the slow-roll corrections.

We can understand a background dynamics of the gauge field from this effective potential. Let us focus on the coefficient of the Q^2 term. Before inflation occurs, we assume that its coefficient was positive and Q is near an origin of its potential. However, we assume that at a certain time $\frac{\dot{I}}{HI} \simeq n \leq -2$ is realized and Q starts to roll down on the potential. Even if ρ_E modifies slow-roll dynamics, $\frac{\dot{I}}{HI} = -2 + \mathcal{O}(\epsilon_H)$ holds due to (38). Therefore, in an early period, Q grows because of the negativity of the Q^2 term. However, Q stops its growth when the nonlinear magnetic Q^4 term becomes important. Moreover, due to the axion-gauge interaction Q^3 term, this effective potential gets two different minimum values, so we expect that there is a trajectory where the gauge field finally settles in a deeper bottom of this potential. At this time, σ and Q obey slow-roll equations

$$3H\dot{\sigma} + W_\sigma = -3\frac{\lambda}{f}(\dot{Q} + HQ)gQ^2, \tag{46}$$

$$\left(1+\frac{2}{3}\frac{\dot{I}}{HI}\right)3H\dot{Q} + 2\left(1+\frac{\dot{I}}{HI}\right)H^2Q + 2g^2Q^3 = \frac{\lambda}{f}\dot{\sigma}\frac{gQ^2}{I^2}. \tag{47}$$

Diagonalizing this system, we have

$$\left(1+\frac{2}{3}\frac{\dot{I}}{HI}+\frac{1}{3}\Lambda^2 m_Q^2\right)3H\dot{\sigma} + \left(1+\frac{2}{3}\frac{\dot{I}}{HI}\right)\left(W_\sigma + 3\frac{\lambda}{f}HgQ^3\right) - 2\left(1+\frac{\dot{I}}{HI}+m_Q^2\right)\frac{\lambda}{f}HgQ^3 = 0, \tag{48}$$

$$\left(1+\frac{2}{3}\frac{\dot{I}}{HI}+\frac{1}{3}\Lambda^2 m_Q^2\right)3H\dot{Q} + \left(1+\frac{\dot{I}}{HI}+\left(\frac{1}{2}\Lambda^2+1\right)m_Q^2\right)2H^2Q + \frac{1}{3I}\Lambda m_Q W_\sigma = 0, \tag{49}$$

where we defined two model parameters

$$\Lambda \equiv \frac{\lambda}{If}Q, \qquad m_Q \equiv \frac{gQ}{H}. \tag{50}$$

If $\Lambda^2 \gg 1$ and $m_Q^2 \gg \Lambda^{-2}$ hold, we get the following results:

$$Q \simeq Q_{\rm min} = -\left(\frac{fW_\sigma}{3\lambda gH}\right)^{1/3}, \tag{51}$$

$$\frac{1}{2}\frac{\lambda}{I^2}\frac{\dot{\sigma}}{fH} \simeq m_Q + \frac{1}{m_Q}\left(1+\frac{\dot{I}}{HI}\right). \tag{52}$$

Remarkably, the background gauge field settles in a minimum value of its effective potential. This is essentially an attractor solution in chromonatural inflation [34]. In our model, however, the condition $\Lambda \gg 1$ and the slow-roll equation (52) can be controlled by the gauge-kinetic function. So, we can realize this slow-roll trajectory for a broad parameter region compared to the original chromonatural inflation. Interestingly, this inflationary dynamics generates parity-violating chiral gravitational waves. We discuss the detail of this mechanism later.

Finally, let us check the evolution of the gauge-kinetic function during this period. In this period, the energy densities of the electric and the magnetic fields are given by

$$\rho_E \simeq \frac{3}{2}I^2H^2Q_{\rm min}^2, \qquad \rho_B \simeq \frac{3}{2}I^2g^2Q_{\rm min}^4 = m_Q^2\rho_E. \tag{53}$$

Hence, if $m_Q \gtrsim 1$ holds, the slow-roll equation for φ reads

$$3H\dot{\varphi} + V_\varphi \simeq 2\frac{I_\varphi}{I}(\rho_E - \rho_B). \tag{54}$$

Substituting Eq. (53) into the above equation, we obtain the time evolution of $I(\varphi)$ as

$$I \simeq \left[\frac{3H^2Q_{\rm min}^2}{4\epsilon_V V}(m_Q^2 - 1) + D_2 a^{-2nV/3H^2}\right]^{-1/2}, \tag{55}$$

where D_2 is a constant of integration. Note that we neglected the terms which are suppressed in the slow-roll approximation. The first term in the parentheses is almost constant. Moreover, when the energy density of the axion becomes dominant in the late stage of inflation $3H^2 \simeq W \gg V$, the second term in the parentheses is also almost constant. Hence, I decreases very slowly.

B. Numerical analysis

As a numerical example, let us show this background dynamics by using the potentials

$$V(\varphi) = \Lambda_\varphi^4 \exp[r\varphi], \tag{56}$$

$$W(\sigma) = \Lambda_\sigma^4\left[1 - \cos\left(\frac{\sigma}{f}\right)\right], \tag{57}$$

where Λ_φ and Λ_σ characterize energy densities of the dilaton and the axion. Here, f is the decay constant, and r is a parameter. It is well known that single-field power-law inflation is in conflict with CMB observations. However, in this model, the background gauge field modifies the slow-roll dynamics, and consequently the tensor-to-scalar ratio is suppressed. Hence, there is a room the model becomes viable for CMB observations as we will discuss later.

In Fig. 1, we plotted the time evolution of the energy density of the gauge field in terms of ϵ_E and ϵ_B and the time evolution of the gauge field $Q(t)$. As you can see, ρ_B catches up with ρ_E after 15 e-folds, and the transition of the

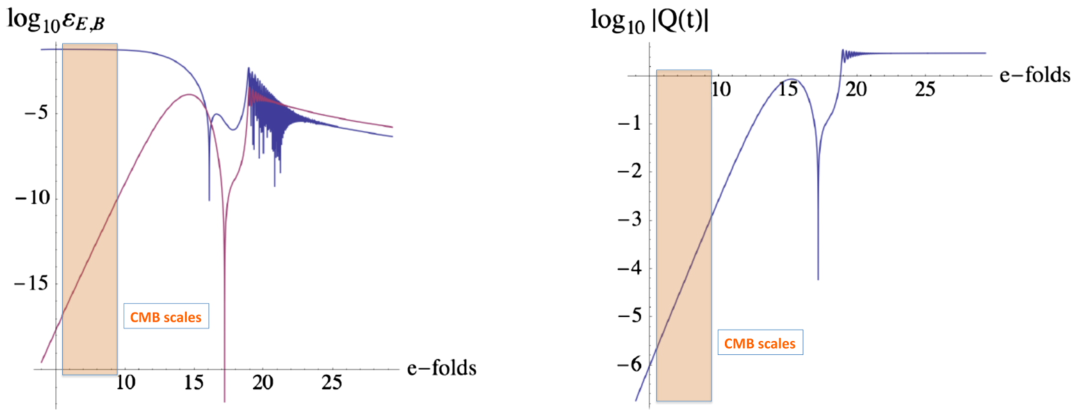

FIG. 1. (Left figure): we plotted time evolutions ϵ_E (blue line) and ϵ_B (red line). Around at 15 e-folds, ρ_B catches up with ρ_E, and the transition of the dynamics of the gauge field happens due to the nonlinear effect. After 20 e-folds, the gauge field settles in an attractor, and both ϵ_E and ϵ_B decrease as I^2. Note that the period when primordial CMB fluctuations are generated is about from 5 to 10 e-folds in this plot. (Right figure): the time evolution of the amplitude of the gauge field $Q(t)$. At first, it continues to grow until 15 e-folds. After the transition, it settles in a constant value. In both figures, we used initial conditions $(\varphi_0, \sigma_0/f) = (4, \pi/3)$ and the parameters $(\Lambda_\varphi, \Lambda_\sigma, r, n, g, \lambda, f) = (10^{-2}, 2\times 10^{-3}, 1, -2.01, 10^{-6}, 10^{-1}, 10)$.

dynamics of the gauge field happens due to the nonlinear effect. We can also see that $Q(t)$ stops its growth and oscillates when the magnetic energy density grows sufficiently and finally settles in a constant value. Note that we used a super-Planckian decay constant $f > M_{\rm pl}$ in the plot by assuming it can be effectively produced by the combination of sub-Planckian decay constants derived from aligned multiple axions [40].

In the next section, we show that, in the late stage of inflation, one of circular polarization states of gauge field fluctuations are enhanced due to the tachyonic instability and the rapid growth of the gauge field produces sizable circularly polarized gravitational waves.

III. CHIRAL GRAVITATIONAL WAVES

In this section, we consider a perturbed universe. To analyze the dynamics, we need to define perturbed quantities. First, for the metric, we use the variables

$$N = 1 + 2\phi, \qquad N_i = \partial_i \beta + \beta_i, \qquad q_{ij} = a(t)^2(\delta_{ij} + \gamma_{ij}), \tag{58}$$

where the spatial metric is further decomposed as

$$\gamma_{ij} = -2\psi\delta_{ij} + 2E_{,ij} + 2W_{(i,j)} + h_{ij}. \tag{59}$$

Note that β_i and W_i are transverse vectors and h_{ij} is a transverse traceless tensor. We choose the flat-slicing gauge

$$\psi = E = W_i = 0. \tag{60}$$

Next, we decompose the non-Abelian gauge field as

$$A^a_0 = a(t)[\partial_a Y + Y_a], \tag{61}$$

$$A^a_i = a(t)[(Q(t) + \delta Q)\delta_{ai} + \epsilon_{iac}(\partial_c U + U_c) + \partial_i(\partial_a M + M_a) + T_{ai}], \tag{62}$$

where Y_a, U_a, and M_a are transverse vectors and T_{ai} is a transverse traceless tensor. Here, we did not discriminate between the index a and the spatial index i. This is allowed because the diagonal transformation of SU(2) and the rotation SO(3) remains the symmetry in the background. Remarkably, not only scalar and vector but also tensor perturbations exist. As is usual, scalar, vector, and tensor perturbations are decoupled at the linear level. We will see that Y and Y_a are nondynamical variables.

Because of SU(2) gauge symmetry, there is the gauge transformation

$$A^a_\mu \to A^a_\mu + g^{-1}\partial_\mu \alpha^a + \epsilon^{abc} A^b_\mu \alpha^c, \tag{63}$$

where α^a are gauge parameters. We can eliminate 3 degrees of freedom using this gauge freedom. So, we fix its gauge by setting

$$M = M_a = 0. \tag{64}$$

Finally, we decompose (pseudo)scalar fields into their background and perturbation variables

$$\varphi = \bar{\varphi}(t) + \delta\varphi,$$
$$\sigma = \bar{\sigma}(t) + \delta\sigma. \tag{65}$$

A. Tensor perturbation dynamics

Let us analyze the dynamics of tensor perturbations in this model. Using a new variable $\psi_{ij} \equiv a(\tau)h_{ij}$, the quadratic action S_{EH} for tensor perturbations is given by

$$\delta S_{\mathrm{EH}} = \int d\boldsymbol{x} d\tau \frac{1}{2}\left[\frac{1}{4}\psi'^{ij}\psi'_{ij} - \frac{1}{4}\psi^{ij,k}\psi_{ij,k} - \left(\frac{3}{4}\frac{a''}{a} - \frac{1}{2}\left(\frac{a'}{a}\right)^2\right)\psi^{ij}\psi_{ij}\right], \tag{66}$$

where a prime represents a derivative with respect to a conformal time τ. We also have contributions to the quadratic action for tensor perturbations from the (pseudo)scalar actions as

$$\delta S_{\mathrm{dilaton}} + \delta S_{\mathrm{axion}} = \int d\boldsymbol{x} d\tau \left(-\frac{a^2}{4}\psi^{ij}\psi_{ij}\right) \times \left[\frac{1}{2a^2}(\bar{\varphi}'^2 + \bar{\sigma}'^2) - V(\bar{\varphi}) - W(\bar{\sigma})\right]. \tag{67}$$

Moreover, using a new variable $t_{ai} \equiv a(\tau)I(\bar{\varphi})T_{ai}$, we obtain the quadratic actions for the tensor perturbations from the gauge sector

$$\begin{aligned}\delta S_{\mathrm{gauge}} = \int d\boldsymbol{x} d\tau \left(-\frac{1}{4}\right)\Bigg[&-I^2\frac{(aQ)'^2}{2a^2}\psi^{ij}\psi_{ij} + \frac{3}{2}a^2I^2g^2Q^4\psi^{ij}\psi_{ij} - 2\left(t'^a_i t'^a_i + \frac{I''}{I}t^a_i t^a_i\right) \\ &+ 2t^a_{i,j}t^a_{i,j} - 4agQ\epsilon^{abi}t^b_j t^a_{j,i} \\ &+ \frac{4I}{a}(aQ)'\psi^{ij}\left(t'_{ij} - \frac{I'}{I}t_{ij}\right) - 4aIgQ^2\psi^{jm}\epsilon^a_{ij}t^a_{m,i} \\ &- 4a^2Ig^2Q^3\psi^{ij}t_{ij}\Bigg]\end{aligned} \tag{68}$$

and that from the Chern-Simons sector

$$\delta S_{\mathrm{CS}} = \int d\boldsymbol{x} d\tau \frac{1}{2I^2}\frac{\lambda}{f}\bar{\sigma}'(\epsilon^{ijk}t^a_i t^a_{k,j} - agQt^{ij}t_{ij}). \tag{69}$$

Using the slow-roll parameters and the approximate scale factor

$$a(\tau) \simeq -\frac{1}{H\tau}, \tag{70}$$

we can write the total quadaratic action for tensor perturbations at the second order as

$$\begin{aligned}\delta S_{\mathrm{tensor}} &\equiv \delta S_{\mathrm{EH}} + \delta S_{\mathrm{scalar}} + \delta S_{\mathrm{gauge}} + \delta S_{\mathrm{CS}} \\ &= \int d^3\boldsymbol{x} d\tau \frac{1}{2}\left[\frac{1}{4}\psi'^{ij}\psi'_{ij} - \frac{1}{4}\psi^{ij,k}\psi_{ij,k} + \frac{1}{2\tau^2}\psi^{ij}\psi_{ij}\right] \\ &\quad + \int d^3\boldsymbol{x} d\tau\left[\frac{1}{2}t'^a_i t'^a_i - \frac{1}{2}t^a_{i,j}t^a_{i,j} + \frac{1}{2}\left(\frac{I''}{I} - \frac{2m_Q\xi}{\tau^2}\right)t^a_i t^a_i - \frac{1}{\tau}(m_Q + \xi)\epsilon^{ijk}t^a_i t^a_{k,j}\right] \\ &\quad + \int d^3\boldsymbol{x} d\tau\left[\frac{\sqrt{\epsilon_E}}{\tau}\psi^{ij}\left(t'_{ij} - \frac{I'}{I}t_{ij}\right) - \frac{\sqrt{\epsilon_B}}{\tau}\psi^{jm}\epsilon^a_{ij}t^a_{m,i} + \frac{\sqrt{\epsilon_B}m_Q}{\tau^2}\psi^{ij}t_{ij} + \frac{\epsilon_E - \epsilon_B}{4\tau^2}\psi^{ij}\psi_{ij}\right],\end{aligned} \tag{71}$$

where we defined a new variable,

$$\xi \equiv \frac{\lambda}{2I^2}\frac{\dot{\bar{\sigma}}}{fH}. \tag{72}$$

We shall use the interaction picture. We treat ψ_{ij} and t_{ij} as free fields in the de Sitter background at the leading order. We can regard the last line in the action (71) as the interaction part. To calculate the power spectrum of gravitational waves, we quantize these variables. The canonical quantization gives rise to the expansion

$$\psi_{ij}(\boldsymbol{x},\tau) = 2\sum_{A=\pm}\int\frac{d^3\boldsymbol{k}}{(2\pi)^3}\hat{\psi}^A_k(\tau)e^{i\boldsymbol{k}\cdot\boldsymbol{x}}, \tag{73}$$

$$= 2\sum_{A=\pm}\int\frac{d^3\boldsymbol{k}}{(2\pi)^3}[e^A_{ij}(\hat{\boldsymbol{k}})\psi^A_k(\tau)a^A_{\boldsymbol{k}} + e^{A*}_{ij}(-\hat{\boldsymbol{k}})\psi^{A*}_k(\tau)a^{A\dagger}_{-\boldsymbol{k}}]e^{i\boldsymbol{k}\cdot\boldsymbol{x}}, \tag{74}$$

$$t_{ij}(\boldsymbol{x},\tau) = 2\sum_{A=\pm}\int\frac{d^3\boldsymbol{k}}{(2\pi)^3}\hat{t}^A_k(\tau)e^{i\boldsymbol{k}\cdot\boldsymbol{x}}, \tag{75}$$

$$= \sum_{A=\pm}\int\frac{d^3\boldsymbol{k}}{(2\pi)^3}[e^A_{ij}(\hat{\boldsymbol{k}})t^A_k(\tau)b^A_{\boldsymbol{k}} + e^{A*}_{ij}(-\hat{\boldsymbol{k}})t^{A*}_k(\tau)b^{A\dagger}_{-\boldsymbol{k}}]e^{i\boldsymbol{k}\cdot\boldsymbol{x}}, \tag{76}$$

where $e^A_{ij}(\hat{\boldsymbol{k}})$ are the polarization tensors which satisfy the following normalization relation, $e^{Aij}(\hat{\boldsymbol{k}})e^B_{ij}(-\hat{\boldsymbol{k}}) = \delta^{AB}$, and the index "$A = \{+,-\}$" represents a circular polarization state defined by $ik^i\epsilon^a_{ij}e^{\pm}_{jm}(\hat{\boldsymbol{k}}) = \pm ke^{\pm}_{am}(\hat{\boldsymbol{k}})$. The creation and annihilation operators $a^A_{\boldsymbol{k}}$, $b^A_{\boldsymbol{k}}$ satisfy the following commutation relations:

$$[a_{\boldsymbol{k}}^A, a_{-\boldsymbol{k}'}^{B\dagger}] = [b_{\boldsymbol{k}}^A, b_{-\boldsymbol{k}'}^{B\dagger}] = (2\pi)^3\delta_{AB}\delta^3(\boldsymbol{k}+\boldsymbol{k}'),$$
$$[a_{\boldsymbol{k}}^A, b_{\boldsymbol{k}'}^B] = [a_{\boldsymbol{k}}^A, b_{-\boldsymbol{k}'}^{B\dagger}] = 0. \tag{77}$$

Moreover, ψ_k^A and t_k^A are mode functions which satisfy the following equations of motion in the de Sitter spacetime:

$$\frac{d^2\psi_k^\pm}{dx^2} + \left(1 - \frac{2}{x^2}\right)\psi_k^\pm = 0, \tag{78}$$

$$\frac{d^2 t_k^\pm}{dx^2} + \left(1 - \frac{d^2 I/dx^2}{I} + \frac{2m_Q\xi}{x^2} \mp \frac{2(m_Q+\xi)}{x}\right)t_k^\pm = 0. \tag{79}$$

Here, we used a dimensionless time variable $x \equiv -k\tau$. In the in-in formalism [41], the in state is given by

$$|in\rangle \equiv T\exp\left(-i\int_{-\infty(1+\epsilon)}^{\tau} d\tilde{\tau} H_I(\tilde{\tau})\right)|0\rangle, \tag{80}$$

where T represents the time-ordered product and $|0\rangle$ is a vacuum state defined by

$$a_{\boldsymbol{k}}^A|0\rangle = b_{\boldsymbol{k}}^A|0\rangle = 0, \qquad \langle 0|0\rangle = 1. \tag{81}$$

The interaction Hamiltonian can be read off from the action (71) as

$$H_I(\tau) = -\int d^3\boldsymbol{x}\left[\frac{\sqrt{\epsilon_E}}{\tau}\psi^{ij}v_{ij} - \frac{\sqrt{\epsilon_B}}{\tau}\psi^{jm}\epsilon_{ij}^a t_{m,i}^a + \frac{\sqrt{\epsilon_B}m_Q}{\tau^2}\psi^{ij}t_{ij} + \frac{\epsilon_E - \epsilon_B}{4\tau^2}\psi^{ij}\psi_{ij}\right]$$
$$= -2\sum_{A=\pm}\int\frac{d^3\boldsymbol{k}}{(2\pi)^3}\left[J_{\boldsymbol{k}}^A\psi_{-\boldsymbol{k}}^A + \frac{\epsilon_E-\epsilon_B}{2\tau^2}\psi_{\boldsymbol{k}}^A\psi_{-\boldsymbol{k}}^A\right], \tag{82}$$

where we used new variables,

$$v_{ij} \equiv t'_{ij} - \frac{I'}{I}t_{ij}, \qquad v_{\boldsymbol{k}}^A = t_{\boldsymbol{k}}^A{\prime} - \frac{I'}{I}t_{\boldsymbol{k}}^A, \tag{83}$$

$$J_{\boldsymbol{k}}^\pm(\tau) \equiv \frac{\sqrt{\epsilon_E}}{\tau}v_{\boldsymbol{k}}^\pm + \left(\frac{\sqrt{\epsilon_B}m_Q}{\tau^2} \pm \frac{k\sqrt{\epsilon_B}}{\tau}\right)t_{\boldsymbol{k}}^\pm. \tag{84}$$

The amplitude of a helicity mode of gravitational waves in the in state is given by

$$(2\pi)^3\delta(\boldsymbol{k}+\boldsymbol{k}')\langle in|h_k^A(\tau)^2|in\rangle = \sum_{N=0}^{\infty}(-i)^N\int^{\tau}d\tau_1\int^{\tau_1}d\tau_2\ldots\int^{\tau_{N-1}}d\tau_N \times\langle 0|[[[h_{\boldsymbol{k}}^A(\tau)h_{\boldsymbol{k}'}^A(\tau), H_I(\tau_1)], H_I(\tau_2)]\ldots, H_I(\tau_N)]|0\rangle. \tag{85}$$

Expanding Eq. (85) up to the second order in H_I, we have

$$(85) = \frac{4}{a(\tau)^2}(\langle 0|\psi_{\boldsymbol{k}}^A(\tau)\psi_{\boldsymbol{k}'}^A(\tau)|0\rangle \tag{86}$$

$$-i\int^{\tau}d\tau_1\langle 0|[\psi_{\boldsymbol{k}}^A(\tau)\psi_{\boldsymbol{k}'}^A(\tau), H_I(\tau_1)]|0\rangle \tag{87}$$

$$-\int^{\tau}d\tau_1\int^{\tau_1}d\tau_2\langle 0|[[\psi_{\boldsymbol{k}}^A(\tau)\psi_{\boldsymbol{k}'}^A(\tau), H_I(\tau_1)], H_I(\tau_2)]|0\rangle) \tag{88}$$

$$+\,(\text{higher order}). \tag{89}$$

Using commutation relations (77) and normalization conditions for the polarization tensors, we get

$$(87) = (2\pi)^3\delta(\boldsymbol{k}+\boldsymbol{k}') \times 16H^2\tau^2\,\mathrm{Im}\left[\int^{\tau}d\tau_1\frac{\epsilon_E-\epsilon_B}{\tau_1^2}\psi_k^A(\tau_1)^2\psi_k^{A*}(\tau)^2\right], \tag{90}$$

$$(88) = (2\pi)^3\delta(\boldsymbol{k}+\boldsymbol{k}')\times(-32H^2\tau^2)\int^{\tau}d\tau_1\int^{\tau_1}d\tau_2 \times[G_k(\tau,\tau_1)G_k(\tau,\tau_2)J_k^{A*}(\tau_1)J_k^A(\tau_2) + G_k(\tau,\tau_1)F_k(\tau_1,\tau_2)\psi_k(\tau)\psi_k^*(\tau_2)], \tag{91}$$

where we defined the functions

$$G_k(\tau,\tau_i) \equiv 2i\,\mathrm{Im}[\psi_k(\tau)\psi_k^*(\tau_i)], \tag{92}$$

$$F_k(\tau_1,\tau_2) \equiv 2i\,\mathrm{Im}[J_k^A(\tau_1)J_k^{A*}(\tau_2)] \tag{93}$$

which came from the commutation relations of $\hat{\psi}_{\boldsymbol{k}}^A$ and $\hat{J}_{\boldsymbol{k}}^A$.

As to the mode functions for the metric, we can take the Bunch-Davis (BD) mode functions

$$\psi_k^\pm = \frac{1}{\sqrt{2k}}\left(1+\frac{i}{x}\right)e^{ix}. \tag{94}$$

For the gauge field, it is difficult to give an analytic solution for t_k^A because $I(\bar{\varphi})$, m_Q, and ξ in Eq. (79) are not known analytically. Therefore, we approximately solve t_k^A in each inflationary stage as discussed in Sec. II A and estimate the Gravitational Wave (GW) spectrum analytically in each stage.

B. Tensor spectrum in the early stage of inflation

Let us estimate the GW spectrum in the early stage of inflation. During this stage, m_Q and ξ are negligible so that the equation of motion for $t_k^\pm$ (79) is approximately given by

$$\frac{d^2 t_k^\pm}{dx^2} + \left(1 - \frac{d^2 I/dx^2}{I}\right) t_k^\pm \simeq 0. \tag{95}$$

The time evolution of $I(\bar{\varphi})$ depends on n and an initial value of the gauge field. If the gauge field grows sufficiently, however, we obtain the transient attractor $I \propto a^{-2}$ as we showed in Eq. (38). Therefore, we can approximately calculate

$$\frac{dI/dx}{I} \sim \frac{2}{x}, \qquad \frac{d^2 I/dx^2}{I} \sim \frac{2}{x^2}. \tag{96}$$

Thus, the mode fluctuations for the gauge field in this stage are

$$t_k^\pm \simeq \frac{1}{\sqrt{2k}} \left(1 + \frac{i}{x}\right) e^{ix}. \tag{97}$$

Substituting Eqs. (94) and (97) into Eq. (85), we can evaluate the power spectrum. Here, we use the cosine and sine integrals

$$\mathrm{Ci}(x) \equiv -\int_x^\infty dx \frac{\cos x}{x} = \gamma + \ln x + \mathcal{O}(x^2), \tag{98}$$

$$\mathrm{Si}(x) \equiv \int_0^x dx \frac{\sin x}{x} = x + \mathcal{O}(x^3), \tag{99}$$

where γ is an Euler number. Then, we get

$$(90) \times (16H^2\tau^2)^{-1} = \frac{\epsilon_E - \epsilon_B}{3} \left[\frac{1}{x^2} - \frac{1}{x} \left(\mathrm{Ci}(2x)\sin 2x - \mathrm{Si}(2x)\cos 2x + \frac{\pi}{2}\cos 2x \right) + \frac{x^2 - 1}{2x^2} \left(\mathrm{Ci}(2x)\cos 2x + \mathrm{Si}(2x)\sin 2x - \frac{\pi}{2}\sin 2x \right) \right], \tag{100}$$

and

$$\begin{aligned}
(91) \times (-32H^2\tau^2)^{-1} = &-\frac{\pi^2}{32}\left[\epsilon_E - \frac{4m_Q}{3}\sqrt{\epsilon_E\epsilon_B} + \left(1 + \frac{4m_Q^2}{9}\right)\epsilon_B\right]\left(\frac{x^2+1}{x^2}\right) - \left(\frac{\sqrt{\epsilon_E\epsilon_B}}{4} - \frac{m_Q\epsilon_B}{12}\right)\frac{s_A}{x} \\
&- \left[\frac{13}{12}\epsilon_E - \frac{2m_Q}{3}\sqrt{\epsilon_E\epsilon_B} - \left(\frac{1}{16} - \frac{2m_Q^2}{27}\right)\epsilon_B\right]\frac{1}{x^2} + \left[\frac{11}{12x}\epsilon_E + \left(\frac{s_A}{4} - \frac{2m_Q}{3x} - \frac{3s_A}{8x^2}\right)\sqrt{\epsilon_E\epsilon_B}\right. \\
&\left. - \left(\frac{s_A m_Q}{12} + \frac{1}{8x} - \frac{5m_Q^2}{54x} - \frac{s_A m_Q}{6x^2}\right)\epsilon_B\right]\pi\cos 2x - \left[\left(\frac{2}{3} - \frac{7}{6x^2}\right)\epsilon_E - \left(\frac{1}{3}m_Q + \frac{5s_A}{4x} - \frac{m_Q}{x^2}\right)\sqrt{\epsilon_E\epsilon_B}\right. \\
&\left. - \left(\frac{1}{4} + \frac{m_Q^2}{54} - \frac{s_A m_Q}{2x} + \frac{11m_Q^2}{54x^2}\right)\epsilon_B\right]\left[\mathrm{Ci}(2x)\cos 2x + \mathrm{Si}(2x)\sin 2x - \frac{1}{2}\pi\sin 2x\right] \\
&- \left(\frac{1}{8}\epsilon_E - \frac{1}{6}m_Q\sqrt{\epsilon_E\epsilon_B} + \frac{1}{8}\epsilon_B + \frac{1}{18}m_Q^2\epsilon_B\right)\left(\frac{x^2+1}{x^2}\right)[\mathrm{Ci}(2x)^2 + \mathrm{Si}(2x)^2 - \pi\mathrm{Si}(2x)] \\
&+ \left[\frac{11}{6x}\epsilon_E + \left(\frac{s_A}{2} - \frac{4m_Q}{3x} - \frac{3s_A}{4x^2}\right)\sqrt{\epsilon_E\epsilon_B} - \left(\frac{s_A m_Q}{6} + \frac{1}{4x} - \frac{5m_Q^2}{27x} - \frac{s_A m_Q}{3x^2}\right)\epsilon_B\right] \\
&\times [\mathrm{Ci}(2x)\sin 2x - \mathrm{Si}(2x)\cos 2x] + \mathrm{Re}\left[\left(\frac{\epsilon_E}{4} - \left(\frac{m_Q}{6} + i\frac{s_A}{2}\right)\sqrt{\epsilon_E\epsilon_B} - \left(\frac{1}{4} - i\frac{s_A m_Q}{6}\right)\epsilon_B\right)\right. \\
&\left.\times \left(1 - \frac{2i}{x} - \frac{1}{x^2}\right)e^{-2ix}\int^x dx_1 \frac{1}{x_1}\left(\mathrm{Ci}(2x_1) + i\mathrm{Si}(2x_1) - i\frac{\pi}{2}\right)\right].
\end{aligned} \tag{101}$$

Note that we omitted $(2\pi)^3\delta(\boldsymbol{k} + \boldsymbol{k}')$ in the above results. Moreover, we approximately treated the slow-roll parameters as constants since their time dependence is suppressed by the slow-roll parameters. In the superhorizon limit $x \to 0$, we have

$$\mathcal{P}_h^\pm(k) = \langle in|h_k^\pm(\tau)^2|in\rangle \simeq \frac{2H^2}{k^3}\left[1 + 4\left(\epsilon_E - m_Q\sqrt{\epsilon_E\epsilon_B} + \frac{2}{9}m_Q^2\epsilon_B\right)(\ln x)^2\right]. \tag{102}$$

The power spectrum of the gravitational waves is not constant in the superhorizon due to the interaction with the gauge field. However, its modification will not be so serious unless the duration of this period is too large. This tensor spectrum in this stage is generated around CMB scales, and we can see no parity violation in the spectrum.

C. Chiral gravitational waves in the late stage of inflation

Now, we calculate the spectrum in the late stage of inflation. In this stage, ξ and m_Q contribute the background dynamics. From the slow-roll equation (52), we have

$$\xi \simeq m_Q + \frac{1}{m_Q}\left(1+\frac{\dot{I}}{HI}\right). \tag{103}$$

As to the gauge-kinetic function, it evolves as $x^{-nV/3H^2}$ ($\because$(55)). Hence, we can calculate

$$\frac{dI/dx}{I} \sim -\frac{\boldsymbol{n}}{x}, \quad \frac{d^2I/dx^2}{I} \sim \frac{\boldsymbol{n}(\boldsymbol{n}+1)}{x^2}, \quad \boldsymbol{n} \equiv nV/3H^2 \lesssim 1. \tag{104}$$

Note that the energy density of the axion is greater than that of the dilaton in this stage. Then, Eq. (79) reads

$$\frac{d^2 t_k^{\pm}}{dx^2} + \left(1+\frac{A}{x^2} \mp \frac{2B}{x}\right) t_k^{\pm} \simeq 0, \tag{105}$$

where

$$A \equiv 2\left(m_Q^2 + 1 - \frac{\boldsymbol{n}(\boldsymbol{n}-1)}{2}\right), \qquad B \equiv 2m_Q + \frac{1}{m_Q}(1+\boldsymbol{n}). \tag{106}$$

We can neglect time dependence of A and B. Here, we consider the parameter region where both A and B have positive values. We can see that the mass term of t_k^- is always positive, so this mode is stable. On the other hand, t_k^+ has the tachyonic instability during the time interval

$$\frac{1}{2}\left(B - \sqrt{B^2 - A}\right) < x < \frac{1}{2}\left(B + \sqrt{B^2 - A}\right), \tag{107}$$

and this instability can enhance one of the helicity modes of gravitational waves.

Let us focus on the t_k^+ mode. It is known that solutions are given by Whittaker functions

$$t_k^+(x) = \frac{1}{\sqrt{2k}}\left(C_1 M_{\kappa,\mu}(2ix) + C_2 W_{\kappa,\mu}(2ix)\right), \tag{108}$$

where C_1 and C_2 are constants and

$$\kappa \equiv iB, \qquad \mu^2 \equiv \frac{1}{4} - A. \tag{109}$$

In the subhorizon limit $x \to \infty$, these functions have asymptotic expansion

$$M_{\kappa,\mu}(2ix) \simeq \frac{\Gamma(1+2\mu)}{\Gamma(\frac{1}{2}+\mu-\kappa)}(2i)^{-\kappa} e^{i(x+i\kappa \ln x)} + \frac{\Gamma(1+2\mu)}{\Gamma(\frac{1}{2}+\mu+\kappa)}(-1)^{\frac{1}{2}+\mu-\kappa}(2i)^{\kappa} e^{-i(x+i\kappa \ln x)}, \tag{110}$$

$$W_{\kappa,\mu}(2ix) \simeq (2i)^{\kappa} e^{-i(x+i\kappa \ln x)}. \tag{111}$$

For the mode function to describe the BD vacuum, the constants C_1 and C_2 should be

$$C_1 = \frac{\Gamma(\frac{1}{2}+\mu-\kappa)}{\Gamma(1+2\mu)}(2i)^{\kappa}, \qquad C_2 = -\frac{\Gamma(\frac{1}{2}+\mu-\kappa)}{\Gamma(\frac{1}{2}+\mu+\kappa)}(2i)^{\kappa}(-1)^{\frac{1}{2}+\mu-\kappa}. \tag{112}$$

Now, we can calculate the power spectrum of gravitational waves in this stage. The dominant contribution comes from an integration (91) where the gauge field fluctuations experience the tachyonic instability near the horizon crossing. In this region, the Whittaker M function is a decaying mode and irrelevant for the integration. Moreover, during this stage, we can regard the complex phase of t_k^+ as nearly constant due to its enhancement and approximately treat t_k^+ as a classical variable.[3] As a result, the contribution from $C_1 M_{\kappa,\mu}(2ix)$ and the commutators including $J_{\boldsymbol{k}}^+$ will be numerically negligible. Hence, we can use

$$t_k^+(x) \simeq C_2 W_{\kappa,\mu}(2ix), \tag{113}$$

$$F_k(\tau_1, \tau_2) \simeq 0 \tag{114}$$

in the integration (91). Then, we can evaluate the integration as

$$(91) \simeq (2\pi)^3 \delta(\boldsymbol{k}+\boldsymbol{k}') \times (16H^2\tau^2) \left| \int^{\tau} d\tau_1 G_k(\tau,\tau_1) J_k^A(\tau_1) \right|^2. \tag{115}$$

We can perform this integration by using the identities

$$\int dx x^n e^{ix} W_{\kappa,\mu}(2ix) = \frac{x^{n+1} G^{2,2}_{2,3}\left(2ix \middle| \begin{matrix} -n, & 1+\kappa & \\ \frac{1}{2}-\mu, & \frac{1}{2}+\mu, & -1-n \end{matrix}\right)}{\Gamma(\frac{1}{2}-\kappa-\mu)\Gamma(\frac{1}{2}-\kappa+\mu)}, \tag{116}$$

[3] The detail is discussed in Refs. [17,42].

$$\int dx x^n e^{-ix} W_{\kappa,\mu}(2ix) = x^{n+1} G^{2,1}_{2,3}\left(2ix \middle| \begin{matrix} -n, & 1-\kappa & \\ \frac{1}{2}-\mu, & \frac{1}{2}+\mu, & -1-n \end{matrix}\right), \quad (117)$$

where G is the Meijer G function. Thus, we get the GW power spectrum. For the stable circular polarization state, we obtain the conventional spectrum

$$\mathcal{P}_h^-(k) = \langle in|h_k^-(\tau)^2|in\rangle \simeq \frac{2H^2}{k^3}. \quad (118)$$

For the other circular polarization state, due to the enhancement of the gauge field fluctuations, we have

$$\begin{aligned}\mathcal{P}_h^+(k) &= \langle in|h_k^+(\tau)^2|in\rangle \\ &= \frac{2H^2}{k^3}[1+8|C_2|^2|\sqrt{\epsilon_E}\mathcal{I}_0(m_Q) - \sqrt{\epsilon_B}\mathcal{I}_1(m_Q) + (\boldsymbol{n}\sqrt{\epsilon_E}+m_Q\sqrt{\epsilon_B})\mathcal{I}_2(m_Q)|^2] \\ &\simeq \frac{2H^2}{k^3}[1+8|C_2|^2 Q_{\rm min}^2|\mathcal{I}_0(m_Q) - m_Q\mathcal{I}_1(m_Q)+m_Q^2\mathcal{I}_2(m_Q)|^2], \end{aligned} \quad (119)$$

where we defined

$$\mathcal{I}_0(m_Q) = \frac{i\Gamma(-\frac{3}{2}-\mu)\Gamma(-\frac{3}{2}+\mu)}{2}\left(\frac{(\frac{1}{4}-\mu^2-4\kappa)(\frac{9}{4}-\mu^2)+8\kappa(1+\kappa)}{\Gamma(1-\kappa)} - \frac{(\frac{1}{4}-\mu^2+4\kappa)(\frac{9}{4}-\mu^2)-8\kappa(1-\kappa)}{\Gamma(\frac{1}{2}-\mu-\kappa)\Gamma(\frac{1}{2}+\mu-\kappa)\Gamma(-\kappa)^{-1}}\right), \quad (120)$$

$$\mathcal{I}_1(m_Q) = \frac{\Gamma(-\frac{1}{2}-\mu)\Gamma(-\frac{1}{2}+\mu)}{2}\left(\frac{\frac{1}{4}-\mu^2-2\kappa}{\Gamma(1-\kappa)} + \frac{\frac{1}{4}-\mu^2+2\kappa}{\Gamma(\frac{1}{2}-\mu-\kappa)\Gamma(\frac{1}{2}+\mu-\kappa)\Gamma(-\kappa)^{-1}}\right), \quad (121)$$

$$\mathcal{I}_2(m_Q) = i\Gamma\left(-\frac{1}{2}-\mu\right)\Gamma\left(-\frac{1}{2}+\mu\right)\left(\frac{1-2(1+\kappa)(\frac{1}{4}-\mu^2)}{\Gamma(-\kappa)} + \frac{1-2(1-\kappa)(\frac{1}{4}-\mu^2)}{\Gamma(\frac{1}{2}-\mu-\kappa)\Gamma(\frac{1}{2}+\mu-\kappa)\Gamma(1-\kappa)^{-1}}\right). \quad (122)$$

We plotted the ratio of spectra (118) and (119) in Fig. 2. We can see that chiral gravitational waves are more enhanced as m_Q is increasing. This qualitative feature is the same as that of chromonatural inflation [24].

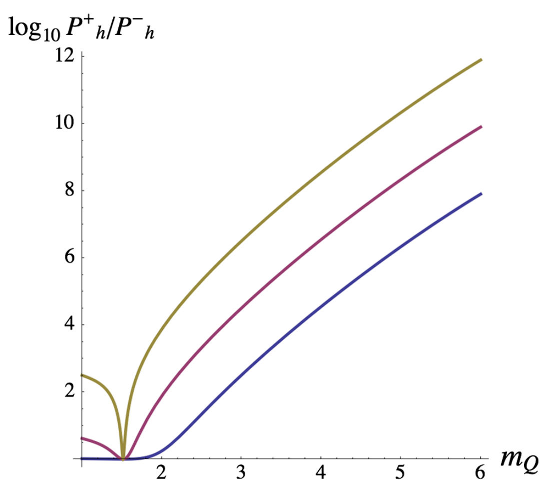

FIG. 2. The behavior of the ratio of the GW spectra as a function of m_Q for $Q_{\rm min} = 10^{-2}$ (blue line), $Q_{\rm min} = 10^{-1}$ (red line), and $Q_{\rm min} = 1$ (yellow line).

Remarkably, this model can avoid the overproduction of chiral gravitational waves on CMB scales discussed in previous works [22,24] and produce sizable circularly polarized gravitational waves on small scales. In the next section, we also study the dynamics of scalar perturbations and show that this model is stable under the scalar fluctuations and consistent with the CMB data.

IV. VIABILITY OF THE MODEL

In this section, we check the dynamics of scalar perturbations. Specifically, we compute the curvature perturbation and its spectrum in the early stage of inflation where fluctuations on CMB scales are created. Moreover, we discuss the stability of scalar perturbations in the late stage of inflation.

Let us derive the quadratic action for scalar perturbations. The Einstein-Hilbert action gives

$$\delta S_{\rm EH} = \int d\tau d\boldsymbol{x}[-12a^4H^2\phi^2 - 4a^2H\phi\partial^2\beta], \quad (123)$$

where ϕ and β are perturbed lapse and shift functions defined in (58). The (pseudo)scalar quadratic actions are given by

$$\delta S_{\rm dilaton} = \int d\tau d\boldsymbol{x}\left[2a^4\dot{\bar\varphi}^2\phi^2 - 2\phi(a^3\dot{\bar\varphi}\delta\varphi' + a^4V_{\bar\varphi}\delta\varphi) + a^2\dot{\bar\varphi}\beta\partial^2\delta\varphi + \frac{1}{2}a^2\delta\varphi'^2 + \frac{1}{2}a^2\delta\varphi\partial^2\delta\varphi - \frac{1}{2}a^4V_{\bar\varphi\bar\varphi}\delta\varphi^2\right],$$

$$\delta S_{\rm axion} = \int d\tau d\boldsymbol{x}\left[2a^4\dot{\bar\sigma}^2\phi^2 - 2\phi(a^3\dot{\bar\sigma}\delta\sigma' + a^4W_{\bar\sigma}\delta\sigma) + a^2\dot{\bar\sigma}\beta\partial^2\delta\sigma + \frac{1}{2}a^2\delta\sigma'^2 + \frac{1}{2}a^2\delta\sigma\partial^2\delta\sigma - \frac{1}{2}a^4W_{\bar\sigma\bar\sigma}\delta\sigma^2\right]. \quad (124)$$

For the quadratic action $\delta S_{\rm gauge}$, we split it into two parts $\delta S^{\rm I}_{\rm gauge} + \delta S^{\rm II}_{\rm gauge}$: the former one includes only gauge field fluctuations

$$\delta S^{\rm I}_{\rm gauge} = \int d\tau d\boldsymbol{x} I^2\left[\frac{3}{2}(a\delta Q)'^2 - (aU)'\partial^2(aU)' + \frac{1}{2}a^4Y\partial^4Y - a^6g^2Q^2Y\partial^2Y \right.$$
$$- a^2Y\left(\partial^2(a\delta Q)' + 2agQ\partial^2(aU)' - 2a^3\frac{(\dot{aQ})}{a}g\partial^2U\right) + a^2\delta Q\partial^2\delta Q - a^2\delta U\partial^4\delta U - 6a^3gQ\delta Q\partial^2U$$
$$\left. - a^4g^2Q^2(9\delta Q^2 - 2U\partial^2U)\right], \quad (125)$$

and the latter one has the interaction with other fields,

$$\delta S^{\rm II}_{\rm gauge} = \int d\tau d\boldsymbol{x}\left[4a^4\rho_E\phi^2 - \frac{2}{3}a^2\rho_B\beta\partial^2\beta - 4a^4\phi\frac{I_{\bar\varphi}}{I}(\rho_E+\rho_B)\delta\varphi + 2\beta aI^2\left(\frac{(\dot{aQ})}{a}a\partial^2\delta Q + gQ^2(a\partial^2U)' + a^3g^2Q^3\partial^2Y\right.\right.$$
$$\left. - \frac{(\dot{aQ})}{a}a^2gQ\partial^2U\right) - 2a^2I^2\left(\phi - \frac{I_{\bar\varphi}}{I}\delta\varphi\right)\frac{(\dot{aQ})}{a}(3(a\delta Q)' - a^2\partial^2Y) - 4a^3I^2\left(\phi + \frac{I_{\bar\varphi}}{I}\delta\varphi\right)gQ^2(3agQ\delta Q + \partial^2U)$$
$$\left. + \left(\frac{I_{\bar\varphi\bar\varphi}}{I} + \frac{I^2_{\bar\varphi}}{I^2}\right)(\rho_E - \rho_B)a^4\delta\varphi^2\right]. \quad (126)$$

Finally, the quadratic action $\delta S_{\rm CS}$ reads

$$\delta S_{\rm CS} = \int ad\tau d\boldsymbol{x}\left[\frac{\lambda\dot{\bar\sigma}}{f}(2\delta Q\partial^2U + agQ(3\delta Q^2 - U\partial^2U))\right.$$
$$\left. + \frac{\lambda}{f}(Ya^2gQ^2\partial^2\delta\sigma + 6agQ^2\delta\sigma'\delta Q - 2(\dot{aQ})\delta\sigma\partial^2U)\right]. \quad (127)$$

A. Curvature perturbation spectrum in the early stage of inflation

The curvature perturbations in the uniform density gauge is defined by [43]

$$-\zeta \equiv \psi + \frac{H}{\dot{\bar\rho}}\delta\rho, \quad (128)$$

where we defined the energy density of matter fields as $\rho = \bar\rho + \delta\rho$. The energy-momentum tensor of matter is given by

$$T_{\mu\nu} = -\frac{2}{\sqrt{-g}}\frac{\delta S_{\rm matter}}{\delta g^{\mu\nu}} \quad (129)$$

$$\equiv (\rho + P)u_\mu u_\nu + Pg_{\mu\nu}, \quad (130)$$

where P is the pressure of matter and $u^\mu = \frac{dx^\mu}{d\tau}$ is the 4-velocity which satisfies

$$u^\mu u_\mu = -1. \quad (131)$$

Therefore, the background energy density reads

$$\bar\rho = -\bar T^0_0$$
$$= \frac{1}{2}\dot{\bar\varphi}^2 + V(\bar\varphi) + \frac{1}{2}\dot{\bar\sigma}^2 + W(\bar\sigma) + \rho_E + \rho_B, \quad (132)$$

and its fluctuation at the first order is given by

$$\delta\rho = -\delta T^0_0 \quad (133)$$

$$\equiv \delta\rho_{\rm dilaton} + \delta\rho_{\rm axion} + \delta\rho_{\rm gauge}, \quad (134)$$

where we split $\delta\rho$ into three variables in the second line, which are derived from each action $S_{\rm dilaton}$, $S_{\rm axion}$, and $S_{\rm gauge}$. More concretely, we have

$$\delta\rho_{\rm dilaton} = \frac{1}{a^2}\bar\varphi'\delta\varphi' + V_{\bar\varphi}\delta\varphi - \frac{2}{a^2}\bar\varphi'^2\phi, \quad (135)$$

$$\delta\rho_{\rm axion} = \frac{1}{a^2}\bar{\sigma}'\delta\sigma' + W_{\bar{\sigma}}\delta\sigma - \frac{2}{a^2}\bar{\sigma}'^2\phi \tag{136}$$

and

$$\begin{aligned}\delta\rho_{\rm gauge} = {}& 6I^2\frac{(a\dot{Q})^2}{a^2}\phi + 3\left(\frac{(a\dot{Q})^2}{a^2} + g^2Q^4\right)II_{\bar{\varphi}}\delta\varphi \\ &+ I^2\frac{(a\dot{Q})}{a}\left(3\frac{(a\dot{\delta Q})}{a} - \partial^2 Y\right) \\ &+ \frac{2}{a}I^2gQ^2\partial^2U + 6I^2g^2Q^3\delta Q.\end{aligned} \tag{137}$$

In the early stage of inflation, the background effect of the magnetic field is negligibly small. So we can set $g=0$ and estimate the power spectrum of the curvature perturbation. We can easily eliminate β and solve ϕ as

$$\phi = \frac{1}{2}\left(\frac{\dot{\bar{\varphi}}}{H}\delta\varphi + \frac{\dot{\bar{\sigma}}}{H}\delta\sigma + 2\frac{(a\dot{Q})}{aH}I^2\delta Q\right). \tag{138}$$

Eliminating Y and defining the variables

$$\delta\varphi = \frac{\Delta_\varphi}{a}, \qquad \delta\sigma = \frac{\Delta_\sigma}{a}, \qquad \delta Q = \frac{\Delta_Q}{\sqrt{2}aI}, \qquad U = \frac{\Delta_U}{\sqrt{2}aI}, \tag{139}$$

we get the quadratic action for scalar perturbations,

$$\begin{aligned}\delta S_{\rm scalar} \equiv {}& \delta S_{\rm EH} + \delta S_{\rm scalar} + \delta S_{\rm gauge} + \delta S_{\rm CS} \\ = {}& \int d^3\boldsymbol{x}d\tau\frac{1}{2}[\Delta_\varphi'^2 + \Delta_\varphi\partial_i^2\Delta_\varphi + \Delta_\sigma'^2 + \Delta_\sigma\partial_i^2\Delta_\sigma + \Delta_Q'^2 + \Delta_Q\partial_i^2\Delta_Q - \Delta_U'\partial_i^2\Delta_U' - \Delta_U\partial_i^4\Delta_U] \\ &- \int d^3\boldsymbol{x}d\tau\frac{1}{2}[M_\varphi^2\Delta_\varphi^2 + M_\sigma^2\Delta_\sigma^2 + M_Q^2\Delta_Q^2 - M_U^2\Delta_U\partial_i^2\Delta_U] + \int d^3\boldsymbol{x}d\tau\left[-2\frac{\sqrt{2\epsilon_E}}{\tau}\frac{I_{\bar{\varphi}}}{I}\Delta_Q'\Delta_\varphi\right] \\ &+ \int d^3\boldsymbol{x}d\tau[M_{\varphi\sigma}\Delta_\varphi\Delta_\sigma + M_{\varphi Q}\Delta_\varphi\Delta_Q + M_{\sigma Q}\Delta_\sigma\Delta_Q - M_{\sigma U}\Delta_\sigma\partial_i^2\Delta_U - M_{QU}\Delta_Q\partial_i^2\Delta_U],\end{aligned} \tag{140}$$

where we defined effective mass parameters

$$M_Q^2 \equiv -\frac{2}{\tau^2} + \frac{\epsilon_E}{\tau^2}(6 - \epsilon_\varphi - \epsilon_\sigma - \epsilon_E), \tag{141}$$

$$M_U^2 \equiv -\frac{2}{\tau^2}, \tag{142}$$

$$\begin{aligned}M_\varphi^2 \equiv {}& -\frac{2}{\tau^2} + \frac{V_{\bar{\varphi}\bar{\varphi}} + \sqrt{2}V_{\bar{\varphi}}\sqrt{\epsilon_\varphi} - H^2(\epsilon_\varphi + \epsilon_\sigma + \epsilon_E)\epsilon_\varphi}{H^2\tau^2} \\ &- \frac{\epsilon_E}{\tau^2}\left(3\frac{I_{\bar{\varphi}\bar{\varphi}}}{I} - \left(\frac{I_{\bar{\varphi}}}{I}\right)^2 - \sqrt{2}\frac{I_{\bar{\varphi}}}{I}\sqrt{\epsilon_\varphi}\right),\end{aligned} \tag{143}$$

$$M_\sigma^2 \equiv -\frac{2}{\tau^2} + \frac{W_{\bar{\sigma}\bar{\sigma}} + \sqrt{2}W_{\bar{\sigma}}\sqrt{\epsilon_\sigma} - H^2(\epsilon_\varphi + \epsilon_\sigma + \epsilon_E)\epsilon_\sigma}{H^2\tau^2} \tag{144}$$

and

$$\begin{aligned}M_{\varphi\sigma} \equiv {}& -\sqrt{\frac{\epsilon_\sigma}{2}}\frac{\epsilon_E I_{\bar{\varphi}}}{\tau^2 I} - \sqrt{\frac{\epsilon_\sigma}{2}}\frac{V_{\bar{\varphi}}}{H^2\tau^2} - \sqrt{\frac{\epsilon_\varphi}{2}}\frac{W_{\bar{\sigma}}}{H^2\tau^2} \\ &+ \frac{\sqrt{\epsilon_\varphi}\sqrt{\epsilon_\sigma}(\epsilon_\sigma + \epsilon_\varphi + \epsilon_E)}{\tau^2},\end{aligned} \tag{145}$$

$$\begin{aligned}M_{\varphi Q} \equiv {}& \sqrt{\frac{\epsilon_E}{2}}\frac{I_{\bar{\varphi}}}{I}\frac{(8 - \epsilon_E)}{\tau^2} + \frac{\sqrt{\epsilon_E\epsilon_\varphi}(-3 + \epsilon_\sigma + \epsilon_\varphi + \epsilon_E)}{\tau^2} \\ &- \sqrt{\frac{\epsilon_E}{2}}\frac{V_{\bar{\varphi}}}{H^2\tau^2},\end{aligned} \tag{146}$$

$$M_{\sigma Q} \equiv \frac{\sqrt{\epsilon_E\epsilon_\sigma}(-3 + \epsilon_\sigma + \epsilon_\varphi + \epsilon_E)}{\tau^2} - \sqrt{\frac{\epsilon_E}{2}}\frac{W_{\bar{\sigma}}}{H^2\tau^2}, \tag{147}$$

$$M_{\sigma U} \equiv -\frac{\lambda}{I^2 f}\frac{\sqrt{2\epsilon_E}}{\tau}, \tag{148}$$

$$M_{QU} \equiv \frac{\xi}{\tau}. \tag{149}$$

Note that in the above calculations we used

$$\frac{I'}{I} \sim \frac{2}{\tau}, \qquad \frac{I''}{I} \sim \frac{2}{\tau^2} \tag{150}$$

and assumed $\dot{\bar{\varphi}}, \dot{\bar{\sigma}} > 0$ so that we could get $\frac{\dot{\bar{\varphi}}}{H} = \sqrt{2\epsilon_\varphi}$ and $\frac{\dot{\bar{\sigma}}}{H} = \sqrt{2\epsilon_\sigma}$. The fluctuation of the energy density is given by

$$\delta\rho = -\frac{1}{a^3}\left[\frac{\sqrt{2\epsilon_\varphi}}{\tau}\Delta'_\varphi + \frac{\sqrt{2\epsilon_\sigma}}{\tau}\Delta'_\sigma + \frac{\sqrt{2\epsilon_E}}{\tau}\left(\Delta'_Q - \frac{2}{\tau}\Delta_Q\right)\right.$$
$$+\left(\frac{\sqrt{2\epsilon_\varphi}}{\tau^2} - a^2 V_{\bar{\varphi}} - \frac{I_{\bar{\varphi}}}{I}\frac{\epsilon_E}{\tau^2}\right)\Delta_\varphi + \left(\frac{\sqrt{2\epsilon_\sigma}}{\tau^2} - a^2 W_{\bar{\sigma}}\right)\Delta_\sigma$$
$$\left. + \frac{\epsilon_\varphi + \epsilon_\sigma - 2\epsilon_E}{\tau^2}(\sqrt{2\epsilon_\varphi}\Delta_\varphi + \sqrt{2\epsilon_\sigma}\Delta_\sigma + \sqrt{2\epsilon_E}\Delta_Q)\right]. \tag{151}$$

To estimate the curvature perturbation at the leading order, let us compare the magnitude of each coefficient (slow-roll parameters) in $\delta\rho$. From the discussion in Sec. II A 1, ϵ_φ and ϵ_E are dominant in the early stage of inflation while ϵ_σ is negligible. Hence, ζ in the flat slicing gauge is approximately given by

$$\zeta \simeq \frac{H\tau^2}{3\sqrt{2\epsilon_\varphi}}(1+\mathcal{E}_E^2)^{-1}\left[\Delta'_\varphi + \mathcal{E}_E\left(\Delta'_Q - \frac{2}{\tau}\Delta_Q\right)\right.$$
$$\left. + 4\frac{1+\mathcal{E}_E^2}{\tau}\Delta_\varphi\right], \tag{152}$$

where we defined a new variable,

$$\mathcal{E}_E \equiv \sqrt{\frac{\epsilon_E}{\epsilon_\varphi}}. \tag{153}$$

We can see that $\mathcal{E}_E$ can be of order unity.

Let us calculate the power spectrum of ζ by using the in-in formalism. We canonically quantize the fields as

$$\Delta_\varphi(\boldsymbol{x},\tau) = \int\frac{d^3\boldsymbol{k}}{(2\pi)^3}\hat{\Delta}_{\varphi\boldsymbol{k}}(\tau)e^{i\boldsymbol{k}\cdot\boldsymbol{x}}$$
$$= \int\frac{d^3\boldsymbol{k}}{(2\pi)^3}[\Delta_{\varphi k}(\tau)c_{\boldsymbol{k}} + \Delta^*_{\varphi k}(\tau)c^\dagger_{-\boldsymbol{k}}]e^{i\boldsymbol{k}\cdot\boldsymbol{x}}, \tag{154}$$

$$\Delta_Q(\boldsymbol{x},\tau) = \int\frac{d^3\boldsymbol{k}}{(2\pi)^3}\hat{\Delta}_{Q\boldsymbol{k}}(\tau)e^{i\boldsymbol{k}\cdot\boldsymbol{x}}$$
$$= \int\frac{d^3\boldsymbol{k}}{(2\pi)^3}[\Delta_{Qk}(\tau)d_{\boldsymbol{k}} + \Delta^*_{Qk}(\tau)d^\dagger_{-\boldsymbol{k}}]e^{i\boldsymbol{k}\cdot\boldsymbol{x}}, \tag{155}$$

where $\Delta_{\varphi k}$ and Δ_{Qk} are mode functions in de Sitter spacetime. From Eq. (140), we can choose mode functions corresponding the BD vacuum as

$$\Delta_{\varphi k} \simeq \frac{1}{\sqrt{2k}}\left(1+\frac{i}{x}\right)e^{ix}, \tag{156}$$

$$\Delta_{Qk} \simeq \frac{1}{\sqrt{2k}}\left(1+\frac{i}{x}\right)e^{ix}. \tag{157}$$

The creation and annihilation operators $c_{\boldsymbol{k}}$ and $d_{\boldsymbol{k}}$ satisfy

$$[c_{\boldsymbol{k}}, c^\dagger_{-\boldsymbol{k}'}] = [d_{\boldsymbol{k}}, d^\dagger_{-\boldsymbol{k}'}] = (2\pi)^3\delta^3(\boldsymbol{k}+\boldsymbol{k}'),$$
$$[c_{\boldsymbol{k}}, d_{\boldsymbol{k}'}] = [c_{\boldsymbol{k}}, d^\dagger_{-\boldsymbol{k}'}] = 0, \tag{158}$$

and the vacuum state is defined by

$$c_{\boldsymbol{k}}|0\rangle = d_{\boldsymbol{k}}|0\rangle = 0, \qquad \langle 0|0\rangle = 1. \tag{159}$$

The interaction Hamiltonian at the leading order reads

$$H_I(\tau) = 4\int d\boldsymbol{x}\left[\frac{\mathcal{E}_E^2}{\tau^2}\Delta_\varphi^2 - \frac{\mathcal{E}_E}{\tau}\left(\Delta'_Q - \frac{2}{\tau}\Delta_Q\right)\Delta_\varphi\right]. \tag{160}$$

Thus, we expect that in the superhorizon limit $x \to 0$ the power spectrum of ζ takes the form

$$\mathcal{P}_\zeta(k) = \langle in|\zeta_k(\tau)^2|in\rangle \simeq \frac{H^2}{4\epsilon_\varphi k^3}(1+\mathcal{A}\mathcal{E}_E^2(\ln x)^2), \tag{161}$$

where $\mathcal{A} \sim \mathcal{O}(10)$ is a numerical factor. Here, note that we neglected the time derivative of slow-roll parameters in the above estimation. This result is consistent with that for dilatonic inflation coupled to a triad of gauge fields [44]. This power spectrum is also not constant in the superhorizon due to the interaction with the gauge field.

B. Scalar perturbation stability in the late stage of inflation

We are interested in the stability conditions of scalar perturbations in the late stage of inflation when the background gauge field settles in the attractor value and chiral gravitational waves are generated. For simplicity, we take the background gauge field function $Q(t)$ to be fixed in the following calculations. Moreover, we neglect the perturbations of the metric and set $\phi = \beta = 0$ because these contributions are suppressed by slow-roll parameters. This truncation is known to be valid from the previous works on the stability of chromonatural inflation [22,24].

After the elimination of Y, we can define the following canonical fieldsL

$$\delta\varphi = \frac{\Delta_\varphi}{a}, \qquad \delta\sigma = \frac{\Delta_\sigma}{a}, \qquad \delta Q = \frac{\Delta_Q}{\sqrt{2}aI},$$
$$U = \frac{1}{\sqrt{2}kaI}\left(\frac{agQ}{k}\Delta_Q + \sqrt{\frac{k^2+2a^2g^2Q^2}{k^2}}\Delta_U\right). \tag{162}$$

We derived the equations of motion for these scalar perturbations in the Appendix. We are interested in the stability condition of scalar perturbations in the region $m_Q \gtrsim \mathcal{O}(1)$ where sizable chiral gravitational waves are produced (see the previous section). For the time window $m_Q \ll x \lesssim \Lambda$, the equations of motion for perturbations at the leading order are given by

$$\frac{d^2\Delta_\varphi}{dx^2} + \left(1 + \frac{4I_{\bar\varphi}^2 Q^2}{x^2}\right)\Delta_\varphi \simeq 0, \tag{163}$$

$$\frac{d^2\Delta_\sigma}{dx^2} + \left(1 + \frac{\Lambda^2 m_Q^2}{x^2}\right)\Delta_\sigma - \frac{5}{\sqrt{2}}\frac{\Lambda m_Q}{x}\frac{d\Delta_Q}{dx} - \frac{\sqrt{2}\Lambda}{x}\Delta_U \simeq 0, \tag{164}$$

$$\frac{d^2\Delta_Q}{dx^2} + \Delta_Q + \frac{5}{\sqrt{2}}\frac{\Lambda m_Q}{x}\frac{d\Delta_\sigma}{dx} \simeq 0, \tag{165}$$

$$\frac{d^2\Delta_U}{dx^2} + \Delta_U - \frac{\sqrt{2}\Lambda}{x}\Delta_\sigma \simeq 0. \tag{166}$$

Note that for the coefficient of gauge-dilaton interactions $I_{\bar\varphi}Q$ we assumed that the background parameter region satisfies $|I_{\bar\varphi}Q| \ll \Lambda$ and neglected them in the above derivation. This assumption can be justified since I needs to become small enough to get a large Λ value, which is proportional to I^{-1}. Hence, dilaton perturbations do not affect the stability on subhorizon scales. To check the stability condition of the scalar dynamics, we focus on one peculiar solution. We use the Wentzel-Kramers-Brillouin (WKB) method for analyzing these equations. Substituting

$$\Delta_\varphi = C_1(x)e^{iS(x)}, \qquad \Delta_\sigma = C_2(x)e^{iS(x)},$$
$$\Delta_Q = C_3(x)e^{iS(x)}, \qquad \Delta_U = C_4(x)e^{iS(x)} \tag{167}$$

into Eqs. (163)–(166), we get

$$\left(1 + \frac{4I_{\bar\varphi}^2 Q^2}{x^2} - S_x^2\right)C_1 \simeq 0, \tag{168}$$

$$\left(1 + \frac{\Lambda^2 m_Q^2}{x^2} - S_x^2\right)C_2 - \frac{5}{\sqrt{2}}\frac{\Lambda m_Q}{x}iS_x C_3 - \frac{\sqrt{2}\Lambda}{x}C_4 \simeq 0, \tag{169}$$

$$(1 - S_x^2)C_3 + \frac{5}{\sqrt{2}}\frac{\Lambda m_Q}{x}iS_x C_2 \simeq 0, \tag{170}$$

$$(1 - S_x^2)C_4 - \frac{\sqrt{2}\Lambda}{x}C_2 \simeq 0, \tag{171}$$

where $S_x \equiv dS/dx = \omega$ is an angular frequency and we neglected the time dependence of $C_i(x)$. Let us focus on the solution with $C_1 = 0$. Then, from Eqs. (169)–(171), we get the relation

$$\left(1 + \frac{\Lambda^2 m_Q^2}{x^2} - \omega^2\right)(1 - \omega^2) - \frac{25}{2}\frac{\Lambda^2 m_Q^2}{x^2}\omega^2 - \frac{2\Lambda^2}{x^2} = 0. \tag{172}$$

Thus, we have two modes:

$$\omega_\pm^2 = \frac{1}{2x^2}\left(2x^2 + \frac{27}{2}\Lambda^2 m_Q^2 \times \left(1 \pm \sqrt{1 + \frac{8x^2}{27\Lambda^2 m_Q^2}\left(\frac{25m_Q^2 + 4}{27m_Q^2}\right)}\right)\right). \tag{173}$$

Recalling that we are considering the region $x \lesssim \Lambda m_Q$, the plus mode ω_+^2 is approximately given by

$$\omega_+^2 \approx \frac{27\Lambda^2 m_Q^2}{2x^2}. \tag{174}$$

Apparently, this mode is positive and stable. On the other hand, for a minus mode ω_-^2, by expanding the square root in Eq. (173) with respect to $x^2/\Lambda^2 m_Q^2$, we get

$$\omega_-^2 \approx \frac{2(m_Q^2 - 2)}{27m_Q^2}. \tag{175}$$

Thus, this mode has the instability in the region $m_Q < \sqrt{2}$. We get the same result as in the previous works [22–24] because the interaction of dilaton perturbations is not dominant in this stage. To confirm this instability, we numerically solved the full scalar equations of motions (A1)–(A4). The time evolution of the scalar fluctuation Δ_φ with several m_Q values is plotted in Fig. 3. We can see that in the region $m_Q < \sqrt{2}$ the instability actually occurs. Therefore, we can avoid the instability by choosing $m_Q > \sqrt{2}$ in the late stage of inflation. Remarkably, in this parameter region, sizable chiral gravitational waves can be generated.

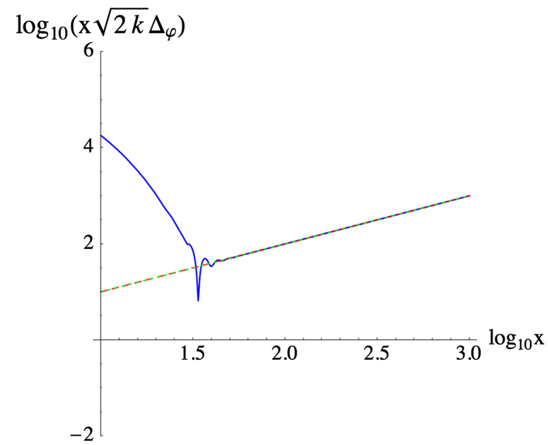

FIG. 3. In this plot, we show the time evolution of $x\sqrt{2k}\Delta_\varphi$ with $m_Q = 1$ (solid blue line), $m_Q = 2$ (dashed red line), and $m_Q = 3$ (dotted green line). The red and green lines are indistinguishable and stable, while the blue line experiences an exponential enhancement due to the instability. Note that we set $(\Lambda, |I_\varphi Q|) \approx (10^2, 10^{-4})$ in this plot.

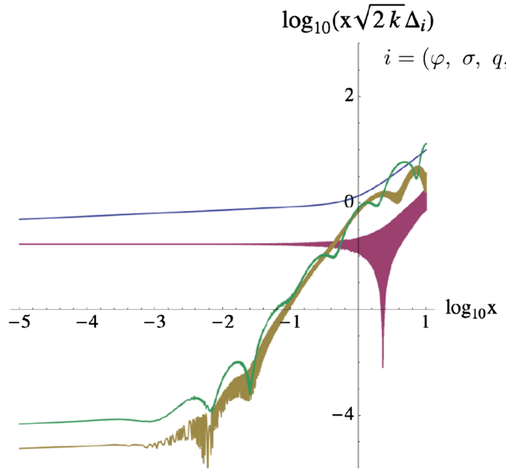

FIG. 4. We plotted the time evolution of $x\sqrt{2k}\Delta_\varphi$ (blue line), $x\sqrt{2k}\Delta_\sigma$ (red line), $x\sqrt{2k}\Delta_q$ (yellow line), and $x\sqrt{2k}\Delta_u$ (green line) in the region $x \lesssim m_Q$. At the horizon crossing, $x\Delta_\varphi$ and $x\Delta_\sigma$ stop decreasing and become constant in the superhorizon due to the expansion of the scale factor. At late times in the superhorizon, this feeds back into the gauge field dynamics and makes their late time behavior constant. Note that we set $(m_Q, \Lambda, |I_\varphi Q|) \approx (2, 10^2, 10^{-4})$ in this plot.

The scalar dynamics in the region $x \lesssim m_Q$ have the similar feature as that of chromonatural inflation [24]. In this region, gauge fluctuations have no instability, and Δ_φ and Δ_σ show the conventional power law behavior. We numerically solved the full scalar equations of motions (A1)–(A4) and plotted the scalar dynamics in the region $x \lesssim m_Q$ in Fig. 4.

V. DISCUSSION

In this section, we discuss constraints from the CMB observations and the possibility of generating chiral gravitational waves in this model.

In Sec. IV A, we estimated the curvature perturbation spectrum on CMB scales. Its dimensionless power spectrum is given by

$$\frac{k^3}{2\pi^2}\mathcal{P}_\zeta(k) \simeq \frac{H^2}{8\pi^2\epsilon_\varphi}(1 + \mathcal{A}\mathcal{E}_E^2(\ln x_f)^2) \tag{176}$$

at the end of inflation $x = x_f$. Primordial fluctuations of the CMB temperature are produced between $-60 \le \ln x_f \le -50$, so the second term is dominant unless $\mathcal{E}_E^2$ is negligibly small. The spectral index n_s at the end of inflation is given by

$$n_s - 1 = \frac{d\ln k^3\mathcal{P}_\zeta}{d\ln k} \simeq \frac{2\mathcal{A}\mathcal{E}_E^2(\ln x_f)}{1 + \mathcal{A}\mathcal{E}_E^2(\ln x_f)^2}. \tag{177}$$

This takes the value $2/(\ln x_f) \sim -0.04$ if the second term in the denominator in (177) is larger than unity. Thus, the spectral index will be nicely consistent with Planck data, even with $\mathcal{E}_E^2 \sim 1$ [3]. Moreover, from the power spectrum of gravitational waves given in Eq. (102), we can estimate the tensor-to-scalar ratio as

$$r = \frac{\mathcal{P}_h^+ + \mathcal{P}_h^-}{\mathcal{P}_\zeta} \simeq 16\epsilon_\varphi^2\frac{\epsilon_\varphi^{-1} + 4\mathcal{E}_E^2(\ln x_f)^2}{1 + \mathcal{A}\mathcal{E}_E^2(\ln x_f)^2} \tag{178}$$

and the spectral tilt of tensor modes at the end of inflation,

$$n_t = \frac{d\ln k^3\mathcal{P}_h^\pm}{d\ln k} \simeq \frac{8\epsilon_E(\ln x_f)}{1 + 4\epsilon_E(\ln x_f)^2}. \tag{179}$$

Note that we neglected the contribution of ϵ_B in Eqs. (178) and (179) since its coefficient m_Q is sufficiently small in this epoch. Remarkably, r can be suppressed by a factor $\epsilon_\varphi/\mathcal{A}$ compared with the conventional single field slow-roll inflation. Moreover, n_t is also red but much closer to the scale invariance than that of scalar perturbations if $\mathcal{E}_E^2$ is sufficiently small. Therefore, without any difficulty, we can choose the appropriate $\mathcal{E}_E^2$ and make the model consistent with the CMB constraints. Though we have not calculated the bispectrum of curvature perturbations nor checked the qualitative features of non-Gaussianity, we expect that its constraint is not so strong unless the axion-gauge interactions are dominant on CMB scales [45].

The most remarkable prediction in this model is that primordial chiral gravitational waves are generated on small scales, which happens after 25 e-folds in our numerical example (see Fig. 1). The frequencies of gravitational waves corresponding to CMB scales are around 10^{-18} Hz today [46], so chiral gravitational waves in our model can be detectable by gravitational wave interferometers of which the sensitivity peaks are located above nHz frequency regions. From the discussion in Sec. III, the ratio of the amplitude of the gravitational wave spectrum is approximately given by

$$\frac{\mathcal{P}_h^+(k)}{\mathcal{P}_h^-(k)} \simeq \begin{cases} 1 & (f \lesssim \mathrm{nHz}) \\ 1 + 8|C_2|^2 Q_{\min}^2|\mathcal{I}_0(m_Q) - m_Q\mathcal{I}_1(m_Q) + m_Q^2\mathcal{I}_2(m_Q)|^2 & (f \gtrsim \mathrm{nHz}) \end{cases}, \tag{180}$$

where $f = \frac{k}{2\pi}$ is the frequency of gravitational waves today. We expect that these two branches are smoothly connected at the transition epoch of two inflationary stages ($f \sim$ nHz).

Finally, let us estimate the intensity of gravitational waves in this model. The intensity derived for vacuum fluctuations is given by [46]

$$h_0^2\Omega_{\rm vac}(f) \simeq 10^{-13}\left(\frac{H}{10^{-4}}\right)^2. \tag{181}$$

Considering CMB normalization in Eq. (176), the Hubble parameter can be estimated as $10^{-7} \lesssim H \lesssim 10^{-5}$ for a certain $\mathcal{E}_E^2$ region; then, $h_0^2\Omega_{\rm vac}$ satisfies $10^{-19} \lesssim h_0^2\Omega_{\rm vac}(f) \lesssim 10^{-15}$. In the late stage of inflation, the enhancement of chirality from the vacuum case is like Fig. 2, getting a large value as m_Q increases, so there are some sets of the parameter region $(Q_{\rm min}, m_Q)$ where chiral gravitational waves can be observed by various detectors such as DECIGO ($h_0^2\Omega_{\rm GW} \gtrsim 10^{-20}$) [36], eLISA ($h_0^2\Omega_{\rm GW} \gtrsim 10^{-10}$) [37], and SKA ($h_0^2\Omega_{\rm GW} \gtrsim 10^{-14}$) [38].

VI. CONCLUSION

In this paper, we studied an inflationary dynamics with a dilaton and an axion coupled to a SU(2) gauge field. Specifically, inspired by supergravity, we introduced a nontrivial gauge-kinetic function to chromonatural inflation [34]. Consequently, the effective coupling constant of the axion to the gauge field is dynamically controlled. For the initial conditions, we required that the gauge field is near the origin of its effective potential and the dilaton playing a role of inflaton initially is energetically dominant. Since the interaction of the axion to the gauge field is sufficiently small, we could neglect the axion in the background dynamics on CMB scales. We derived the power spectrum of scalar and tensor perturbations in this early stage of inflation by using the in-in formalism and discussed its observational implication by looking at the spectral index and the tensor-to-scalar ratio. We found that they are characterized by the kinetic energy density of the gauge field and can be controlled so that the model becomes consistent with the constraints from the current CMB observations. In particular, since the gauge field is inert in the early stage of inflation, the model does not show any conflict with the CMB constraints.

The main prediction of this paper is the generation of chiral gravitational waves on small scales. We found an inflationary solution where the gauge field grows due to the gauge-kinetic function and finally settles in a finite value $Q_{\rm min}$, which realizes the delayed chromonatural inflation. Then, we analyzed tensor dynamics in the late stage of inflation and computed gravitational wave spectrum by employing the in-in formalism and got the qualitatively similar result as chromonatural inflation [24]. The general feature of tensor perturbations is the enhancement of chiral gravitational waves which is controlled by an attractor value $Q_{\rm min}$ and the mass parameter of the gauge field m_Q. Moreover, we checked the stability condition of scalar dynamics and showed that there is a stable parameter region $m_Q > \sqrt{2}$. Note that during this period we have chosen the gauge-kinetic function so that the interaction of the dilaton to the gauge field does not contribute to perturbation dynamics. We found that there is a parameter region where chiral gravitational waves are produced in an interesting frequency range, higher than nHz, which might be detectable in future gravitational wave interferometers and pulsar-timing arrays, such as DECIGO, eLISA, and SKA.

It is interesting to investigate the reheating stage in this model. We expect from our previous work [25] that at this epoch the effective mass parameter m_Q grows and then chiral gravitational waves are more enhanced, which might reach the current observational bounds on ground-based interferometers. In this paper, we studied our model with an isotropic initial condition. Notice that the anisotropy remains in models with a gauge-kinetic function for a non-Abelian gauge field [11], while, in the case of chromonatural inflation, the initial anisotropy decays, and the isotropic configuration is stable [47]. Thus, it is intriguing to investigate the fate of the initial anisotropy in our model. We leave these issues for future work.

ACKNOWLEDGMENTS

We would like to thank P. Adshead and M. Wyman for fruitful notebook and discussion. This work was supported by JSPS KAKENHI Grant No. 25400251, MEXT KAKENHI Grant No. 26104708, and MEXT KAKENHI Grant No. 15H05895.

APPENDIX: EQUATIONS OF MOTION FOR SCALAR PERTURBATIONS

In this Appendix, we list the full equations of motion used for numerical calculations. We set $\phi = \beta = 0$. Then, we have the following equations of motions for scalar perturbations:

$$\frac{d^2\Delta_Q}{dx^2} + \mathcal{Q}_1\Delta_Q + \mathcal{Q}_2\Delta_U + \mathcal{Q}_3\frac{d\Delta_\varphi}{dx} + \mathcal{Q}_4\Delta_\varphi + \mathcal{Q}_5\frac{d\Delta_\sigma}{dx} + \mathcal{Q}_6\Delta_\sigma = 0, \tag{A1}$$

$$\frac{d^2\Delta_U}{dx^2} + \mathcal{U}_1\Delta_U + \mathcal{U}_2\Delta_Q + \mathcal{U}_3\frac{d\Delta_\varphi}{dx} + \mathcal{U}_4\Delta_\varphi + \mathcal{U}_5\frac{d\Delta_\sigma}{dx} + \mathcal{U}_6\Delta_\sigma = 0, \tag{A2}$$

$$\frac{d^2\Delta_\varphi}{dx^2} + \mathcal{P}_1\Delta_\varphi + \mathcal{P}_2\Delta_\sigma + \mathcal{P}_3\frac{d\Delta_Q}{dx} + \mathcal{P}_4\Delta_Q + \mathcal{P}_5\frac{d\Delta_U}{dx} + \mathcal{P}_6\Delta_U = 0, \tag{A3}$$

$$\frac{d^2\Delta_\sigma}{dx^2} + \mathcal{S}_1\Delta_\sigma + \mathcal{S}_2\Delta_\varphi + \mathcal{S}_3\frac{d\Delta_Q}{dx} + \mathcal{S}_4\Delta_Q + \mathcal{S}_5\frac{d\Delta_U}{dx} + \mathcal{S}_6\Delta_U = 0. \tag{A4}$$

As for the coefficients $\mathcal{Q}_i (i = 1, \ldots, 6)$, we get

$$\mathcal{Q}_1 = \frac{1}{x^4(x^2+2m_Q^2)}(4m_Q^6 + 2m_Q^4(2 - 2d\ln I/dxx + 5x^2) + (1-(d\ln I/dx)^2)x^6 + 2m_Q^2x^2(1 - d\ln I/dxx + (3-(d\ln I/dx)^2)x^2) - 2\xi(2m_Q^5 + 5m_Q^3x^2 + 2m_Qx^4)) - \frac{d^2I/dx^2}{I} + \frac{(dI/dx)^2}{I^2}, \tag{A5}$$

$$\mathcal{Q}_2 = \frac{1}{x^4(x^2+2m_Q^2)^{3/2}}(8m_Q^7 + 8m_Q^5(1 - d\ln I/dxx) + 2m_Q^3(4 - 4d\ln I/dxx - 3x^2)x^2 + 2m_Q(1 - d\ln I/dxx - x^2)x^4 - \xi(8m_Q^6 + 4m_Q^4x^2 - 2m_Q^2x^4 - x^6)), \tag{A6}$$

$$\mathcal{Q}_3 = -\frac{2\sqrt{2}I_{\bar\varphi}Q}{x}, \tag{A7}$$

$$\mathcal{Q}_4 = \frac{2\sqrt{2}I_{\bar\varphi}Q}{x^2}(1 - d\ln I/dxx + 2m_Q^2) - \frac{2\sqrt{2}QdI_{\bar\varphi}/dx}{x}, \tag{A8}$$

$$\mathcal{Q}_5 = \frac{5}{\sqrt{2}}\frac{\lambda}{If}\frac{Qm_Q}{x}, \tag{A9}$$

$$\mathcal{Q}_6 = \frac{5}{\sqrt{2}}\frac{\lambda}{If}\frac{Qm_Q}{x^2}. \tag{A10}$$

As for $\mathcal{U}_i (i = 1, \ldots, 6)$, we have

$$\mathcal{U}_1 = \frac{1}{x^4(x^2+2m_Q^2)^2}(16m_Q^8 + 16m_Q^6(1 - d\ln I/dxx + 2x^2) + (1-(d\ln I/dx)^2)x^8 + 4m_Q^4x^2(6(1 - d\ln I/dxx) + (6-(d\ln I/dx)^2)x^2) + 2m_Q^2x^4(7 - 4d\ln I/dxx + 2(2-(d\ln I/dx)^2)x^2) - 2\xi(8m_Q^7 + 12m_Q^5x^2 + 6m_Q^3x^4 + m_Qx^6)) - \frac{d^2I/dx^2}{I} + \frac{(dI/dx)^2}{I^2}, \tag{A11}$$

$$\mathcal{U}_2 = \mathcal{Q}_2, \tag{A12}$$

$$\mathcal{U}_3 = \frac{2\sqrt{2}I_{\bar\varphi}Qm_Q}{x(x^2+2m_Q^2)^{1/2}}, \tag{A13}$$

$$\mathcal{U}_4 = -\frac{2\sqrt{2}I_{\bar\varphi}Qm_Q}{x^2(x^2+2m_Q^2)^{3/2}}(4m_Q^4 + 2m_Q^2(1 - d\ln I/dxx - d\ln I_{\bar\varphi}/dxx + 2x^2) + (3 - d\ln I/dxx - d\ln I_{\bar\varphi}/dxx + x^2)x^2), \tag{A14}$$

$$\mathcal{U}_5 = -\frac{\lambda}{If}\frac{\sqrt{2}Qm_Q^2}{x(x^2+2m_Q^2)^{1/2}}, \tag{A15}$$

$$\mathcal{U}_6 = -\frac{\lambda}{If}\frac{\sqrt{2}Q}{x^2(x^2+m_Q^2)^{3/2}}(2m_Q^4 + m_Q^2x^2 + x^4). \tag{A16}$$

Then, as for $\mathcal{P}_i (i = 1, \ldots, 6)$, we have

$$\mathcal{P}_1 = 1 + \frac{1}{x^2}\left(3\left(\frac{I_{\bar\varphi}^2}{I^2} + \frac{I_{\bar\varphi\bar\varphi}}{I}\right)(\epsilon_B - \epsilon_E) - 2 + \frac{V_{\bar\varphi\bar\varphi}}{H^2} + \frac{4I_{\bar\varphi}^2Q^2}{x^2+2m_Q^2}x^2\right), \tag{A17}$$

$$\mathcal{P}_2 = -\frac{\lambda}{If}\frac{2I_{\bar\varphi}Q^2m_Q}{x^2+2m_Q^2}, \tag{A18}$$

$$\mathcal{P}_3 = -\mathcal{Q}_3, \tag{A19}$$

$$\mathcal{P}_4 = \frac{2\sqrt{2}I_{\bar\varphi}Q}{x^2}(2m_Q^2 - d\ln I/dxx), \tag{A20}$$

$$\mathcal{P}_5 = -\mathcal{U}_3, \tag{A21}$$

$$\mathcal{P}_6 = -\frac{2\sqrt{2}I_{\bar{\varphi}}Qm_Q}{x^2(x^2+2m_Q^2)^{3/2}}(4m_Q^4 + 2m_Q^2(-d\ln I/dxx + 2x^2) + (1 - d\ln I/dxx + x^2)x^2). \tag{A22}$$

Finally, as for $\mathcal{S}_i (i = 1, \ldots, 6)$, we have

$$\mathcal{S}_1 = 1 + \frac{1}{x^2}\left(-2 + \frac{W_{\bar{\sigma}\bar{\sigma}}}{H^2} + \frac{\alpha^2}{I^2 f^2}\frac{Q^2 m_Q^2}{x^2+2m_Q^2}x^2\right), \tag{A23}$$

$$\mathcal{S}_2 = \mathcal{P}_2, \tag{A24}$$

$$\mathcal{S}_3 = -\mathcal{Q}_5, \tag{A25}$$

$$\mathcal{S}_4 = \frac{10}{\sqrt{2}}\frac{\alpha}{If}\frac{Qm_Q}{x^2}\left(1 + \frac{1}{2}d\ln I/dxx\right), \tag{A26}$$

$$\mathcal{S}_5 = -\mathcal{U}_5, \tag{A27}$$

$$\mathcal{S}_6 = -\frac{\lambda}{If}\frac{\sqrt{2}Q}{x^2(x^2+2m_Q^2)^{3/2}}(2m_Q^4(2 + d\ln I/dxx) + m_Q^2(3 + d\ln I/dxx)x^2 + x^4). \tag{A28}$$

---

[1] A. H. Guth, The inflationary universe: A possible solution to the horizon and flatness problems, Phys. Rev. D **23**, 347 (1981); A. A. Starobinsky, A new type of isotropic cosmological models without singularity, Phys. Lett. **91B**, 99 (1980); K. Sato, First order phase transition of a vacuum and expansion of the universe, Mon. Not. R. Astron. Soc. **195**, 467 (1981).

[2] P. A. R. Ade *et al.* (BICEP2 and Keck Array Collaborations), BICEP2/Keck Array VI: Improved Constraints On Cosmology and Foregrounds When Adding 95 GHz Data From Keck Array, Phys. Rev. Lett. **116**, 031302 (2016).

[3] P. A. R. Ade *et al.* (Planck Collaboration), Planck 2015 results. XX. Constraints on inflation, arXiv:1502.02114.

[4] M. Yamaguchi, Supergravity based inflation models: A review, Classical Quantum Gravity **28**, 103001 (2011).

[5] A. Maleknejad, M. M. Sheikh-Jabbari, and J. Soda, Gauge fields and inflation, Phys. Rep. **528**, 161 (2013).

[6] M.-a. Watanabe, S. Kanno, and J. Soda, Inflationary Universe with Anisotropic Hair, Phys. Rev. Lett. **102**, 191302 (2009); S. Kanno, J. Soda, and M.-a. Watanabe, Anisotropic power-law inflation, J. Cosmol. Astropart. Phys. 12 (2010) 024.

[7] M. a. Watanabe, S. Kanno, and J. Soda, The nature of primordial fluctuations from anisotropic inflation, Prog. Theor. Phys. **123**, 1041 (2010); A. E. Gumrukcuoglu, B. Himmetoglu, and M. Peloso, Scalar-Scalar, Scalar-Tensor, and Tensor-Tensor Correlators from Anisotropic Inflation, Phys. Rev. D **81**, 063528 (2010); T. R. Dulaney and M. I. Gresham, Primordial power spectra from anisotropic inflation, Phys. Rev. D **81**, 103532 (2010); N. Bartolo, S. Matarrese, M. Peloso, and A. Ricciardone, Anisotropic power spectrum and bispectrum in the $f(\phi)F^2$ mechanism, Phys. Rev. D **87**, 023504 (2013); A. Naruko, E. Komatsu, and M. Yamaguchi, Anisotropic inflation reexamined: Upper bound on broken rotational invariance during inflation, J. Cosmol. Astropart. Phys. 04 (2015) 045.

[8] M.-a. Watanabe, S. Kanno, and J. Soda, Imprints of anisotropic inflation on the cosmic microwave background, Mon. Not. R. Astron. Soc. **412**, L83 (2011); X. Chen, R. Emami, H. Firouzjahi, and Y. Wang, The TT, TB, EB and BB correlations in anisotropic inflation, J. Cosmol. Astropart. Phys. 08 (2014) 027; J. Ohashi, J. Soda, and S. Tsujikawa, Observational signatures of anisotropic inflationary models, J. Cosmol. Astropart. Phys. 12 (2013) 009.

[9] J. Soda, Statistical anisotropy from anisotropic inflation, Classical Quantum Gravity **29**, 083001 (2012); R. Emami, H. Firouzjahi, S. M. S. Movahed, and M. Zarei, Anisotropic inflation from charged scalar fields, J. Cosmol. Astropart. Phys. 02 (2011) 005; R. Emami and H. Firouzjahi, Curvature perturbations in anisotropic inflation with symmetry breaking, J. Cosmol. Astropart. Phys. 10 (2013) 041.

[10] K. Yamamoto, M.-a. Watanabe, and J. Soda, Inflation with multi-vector-hair: The fate of anisotropy, Classical Quantum Gravity **29**, 145008 (2012).

[11] K. Murata and J. Soda, Anisotropic inflation with non-Abelian gauge-kinetic function, J. Cosmol. Astropart. Phys. 06 (2011) 037.

[12] K.-i. Maeda and K. Yamamoto, Inflationary dynamics with a non-Abelian gauge field, Phys. Rev. D **87**, 023528 (2013); Stability analysis of inflation with an SU(2) gauge field, J. Cosmol. Astropart. Phys. 12 (2013) 018.

[13] K. Choi, K. Y. Choi, H. Kim, and C. S. Shin, Primordial perturbations from dilaton-induced gauge fields, J. Cosmol. Astropart. Phys. 10 (2015) 046.

[14] L. Sorbo, Parity violation in the Cosmic Microwave Background from a pseudoscalar inflaton, J. Cosmol. Astropart. Phys. 06 (2011) 003.

[15] N. Barnaby, R. Namba, and M. Peloso, Phenomenology of a pseudo-scalar inflaton: Naturally large nongaussianity, J. Cosmol. Astropart. Phys. 04 (2011) 009.

[16] J. L. Cook and L. Sorbo, Particle production during inflation and gravitational waves detectable by ground-based interferometers, Phys. Rev. D **85**, 023534 (2012); **86**, 069901 (2012).

[17] N. Barnaby, E. Pajer, and M. Peloso, Gauge field production in axion inflation: Consequences for monodromy, non-Gaussianity in the CMB, and gravitational waves at interferometers, Phys. Rev. D **85**, 023525 (2012).

[18] M. M. Anber and L. Sorbo, Non-Gaussianities and chiral gravitational waves in natural steep inflation, Phys. Rev. D **85**, 123537 (2012).

[19] N. Barnaby, J. Moxon, R. Namba, M. Peloso, G. Shiu, and P. Zhou, Gravity waves and non-Gaussian features from particle production in a sector gravitationally coupled to the inflaton, Phys. Rev. D **86**, 103508 (2012).

[20] S. Mukohyama, R. Namba, M. Peloso, and G. Shiu, Blue tensor spectrum from particle production during inflation, J. Cosmol. Astropart. Phys. 08 (2014) 036.

[21] R. Namba, M. Peloso, M. Shiraishi, L. Sorbo, and C. Unal, Scale-dependent gravitational waves from a rolling axion, J. Cosmol. Astropart. Phys. 01 (2016) 041.

[22] E. Dimastrogiovanni and M. Peloso, Stability analysis of chromo-natural inflation and possible evasion of Lyths bound, Phys. Rev. D **87**, 103501 (2013).

[23] P. Adshead, E. Martinec, and M. Wyman, Gauge fields and inflation: Chiral gravitational waves, fluctuations, and the Lyth bound, Phys. Rev. D **88**, 021302 (2013).

[24] P. Adshead, E. Martinec, and M. Wyman, Perturbations in chromo-natural inflation, J. High Energy Phys. 09 (2013) 087.

[25] I. Obata, T. Miura, and J. Soda, Chromo-natural inflation in the axiverse, Phys. Rev. D **92**, 063516 (2015).

[26] S. Saito, K. Ichiki, and A. Taruya, Probing polarization states of primordial gravitational waves with CMB anisotropies, J. Cosmol. Astropart. Phys. 09 (2007) 002.

[27] M. Shiraishi, A. Ricciardone, and S. Saga, Parity violation in the CMB bispectrum by a rolling pseudoscalar, J. Cosmol. Astropart. Phys. 11 (2013) 051.

[28] N. Bartolo, S. Matarrese, M. Peloso, and M. Shiraishi, Parity-violating and anisotropic correlations in pseudoscalar inflation, J. Cosmol. Astropart. Phys. 01 (2015) 027.

[29] R. Kato and J. Soda, Probing circular polarization in stochastic gravitational wave background with pulsar timing arrays, Phys. Rev. D **93**, 062003 (2016).

[30] N. Barnaby and M. Peloso, Large Nongaussianity in Axion Inflation, Phys. Rev. Lett. **106**, 181301 (2011).

[31] P. D. Meerburg and E. Pajer, Observational constraints on gauge field production in axion inflation, J. Cosmol. Astropart. Phys. 02 (2013) 017.

[32] R. Z. Ferreira and M. S. Sloth, Universal constraints on axions from inflation, J. High Energy Phys. 12 (2014) 139.

[33] R. Z. Ferreira, J. Ganc, J. Norea, and M. S. Sloth, On the validity of the perturbative description of axions during inflation, J. Cosmol. Astropart. Phys. 04 (2016) 039.

[34] P. Adshead and M. Wyman, Chromo-Natural Inflation: Natural Inflation on a Steep Potential with Classical Non-Abelian Gauge Fields, Phys. Rev. Lett. **108**, 261302 (2012).

[35] A. Maleknejad and M. M. Sheikh-Jabbari, Gauge-flation: Inflation from non-Abelian gauge fields, Phys. Lett. B **723**, 224 (2013); Non-Abelian gauge field inflation, Phys. Rev. D **84**, 043515 (2011).

[36] N. Seto, S. Kawamura, and T. Nakamura, Possibility of Direct Measurement of the Acceleration of the Universe using 0.1-Hz Band Laser Interferometer Gravitational Wave Antenna in Space, Phys. Rev. Lett. **87**, 221103 (2001); S. Kawamura *et al.*, The Japanese space gravitational wave antenna: DECIGO, Classical Quantum Gravity **28**, 094011 (2011).

[37] P. Amaro-Seoane *et al.*, eLISA/NGO: Astrophysics and cosmology in the gravitational-wave millihertz regime, GW Notes **6**, 4 (2013).

[38] C. L. Carilli and S. Rawlings, Science with the Square Kilometer Array: Motivation, key science projects, standards and assumptions, New Astron. Rev. **48**, 979 (2004); G. Janssen *et al.*, Gravitational wave astronomy with the SKA, *Proc. Sci.*, AASKA14 (2015) 037.

[39] S. Kanno, J. Soda, and M.-a. Watanabe, Cosmological magnetic fields from inflation and backreaction, J. Cosmol. Astropart. Phys. 12 (2009) 009.

[40] J. E. Kim, H. P. Nilles, and M. Peloso, Completing natural inflation, J. Cosmol. Astropart. Phys. 01 (2005) 005.

[41] S. Weinberg, Quantum contributions to cosmological correlations, Phys. Rev. D **72**, 043514 (2005).

[42] N. Barnaby, R. Namba, and M. Peloso, Observable non-gaussianity from gauge field production in slow roll inflation, and a challenging connection with magnetogenesis, Phys. Rev. D **85**, 123523 (2012).

[43] K. A. Malik and D. Wands, Cosmological perturbations, Phys. Rep. **475**, 1 (2009).

[44] K. Yamamoto, Primordial fluctuations from inflation with a triad of background gauge fields, Phys. Rev. D **85**, 123504 (2012).

[45] H. Funakoshi and K. Yamamoto, Primordial bispectrum from inflation with background gauge fields, Classical Quantum Gravity **30**, 135002 (2013).

[46] M. Maggiore, Gravitational wave experiments and early universe cosmology, Phys. Rep. **331**, 283 (2000).

[47] A. Maleknejad, M. M. Sheikh-Jabbari, and J. Soda, Gauge-flation and cosmic no-hair conjecture, J. Cosmol. Astropart. Phys. 01 (2012) 016; A. Maleknejad and E. Erfani, Chromo-natural model in anisotropic background, J. Cosmol. Astropart. Phys. 02 (2014) 016.